Mon. Not. R. Astron. Soc. **347,** 74–94 (2004)

Low-luminosity Type II supernovae: spectroscopic and photometric evolution

A. Pastorello,[1,2,5★] L. Zampieri,[2] M. Turatto,[2] E. Cappellaro,[3] W. P. S. Meikle,[4] S. Benetti,[2] D. Branch,[5] E. Baron,[5] F. Patat,[6] M. Armstrong,[7] G. Altavilla,[2,1] M. Salvo[8] and M. Riello[2,1]

[1]*Dipartimento di Astronomia, Università di Padova, Vicolo dell' Osservatorio 2, I-35122 Padova, Italy*
[2]*INAF – Osservatorio Astronomico di Padova, Vicolo dell' Osservatorio 5, I-35122 Padova, Italy*
[3]*INAF – Osservatorio Astronomico di Capodimonte, Via Moiariello 16, I-80131 Napoli, Italy*
[4]*Astrophysics Group, Blackett Laboratory, Imperial College, Prince Consort Road, London SW7 2BZ*
[5]*Department of Physics and Astronomy, University of Oklahoma, 440 W. Brooke St., Norman, OK 73019, USA*
[6]*European Southern Observatory, Karl-Schwarzschild-Strasse 2, D-85748, Garching bei Munchen, Germany*
[7]*UK Supernova Patrol, British Astronomical Association, Rolvenden, Kent*
[8]*Australian National University, Mount Stromlo Observatory, Cotter Road, Weston ACT 2611, Australia*

Accepted 2003 September 3. Received 2003 August 26; in original form 2003 July 16

ABSTRACT

In this paper we present spectroscopic and photometric observations for four core-collapsed supernovae (SNe), namely SNe 1994N, 1999br, 1999eu and 2001dc. Together with SN 1997D, we show that they form a group of exceptionally low-luminosity events. These SNe have narrow spectral lines (indicating low expansion velocities) and low luminosities at every phase (significantly lower than those of typical core-collapsed supernovae). The very-low luminosity during the ^{56}Co radioactive decay tail indicates that the mass of ^{56}Ni ejected during the explosion is much smaller ($M_{\rm Ni} \approx 2$–8×10^{-3} M$_\odot$) than the average ($M_{\rm Ni} \approx 6$–10×10^{-2} M$_\odot$). Two supernovae of this group (SN 1999br and SN 2001dc) were discovered very close to the explosion epoch, allowing us to determine the lengths of their plateaux ($\approx$100 d) as well as establishing the explosion epochs of the other, less completely observed SNe. It is likely that this group of SNe represent the extreme low-luminosity tail of a single continuous distribution of Type II plateau supernovae events. Their kinetic energy is also exceptionally low. Although an origin from low-mass progenitors has also been proposed for low-luminosity core-collapsed SNe, recent work provides evidence in favour of the high-mass progenitor scenario. The incidence of these low-luminosity SNe could be as high as 4–5 per cent of all Type II SNe.

Key words: supernovae: general – supernovae: individual: SN 1994N – supernovae: individual: SN 1997D – supernovae: individual: SN 1999br – supernovae: individual: SN 1999eu – supernovae: individual: SN 2001dc.

1 INTRODUCTION

It is widely known that the early spectrophotometric evolution of core-collapsed supernovae (CC-SNe) is very heterogeneous (see e.g. Patat et al. 1994). The radius of the progenitor is believed to play a key role in shaping the early light curve. H-rich red giant progenitors with large initial radii are thought to produce Type II plateau supernovae (II-P SNe). Their luminosity remains nearly constant for a relatively long period (plateau phase, lasting $\sim$110–130 d), during which the hydrogen envelope (in free expansion) starts to recombine, releasing its internal energy. The observed length of the plateau phase depends on the mass of the hydrogen envelope (Arnett 1980; Popov 1992).

On the other hand, the unusual early light curve of SN 1987A with a broad maximum about three months after the explosion is largely attributable to its compact progenitor (Arnett 1987; Woosley et al. 1987). The luminosity at early time is dimmer than expected for a 'typical' II-P SN. Then, with expansion, most of the trapped energy from the radioactive decay of Ni is released and the luminosity rises

★E-mail: apastore@merlino.pd.astro.it

producing a broad maximum in the light curve. After the plateau phase is finished, all II-P SNe (including SN 1987A) have a steep drop in luminosity, marking the passage from the photospheric phase to the nebular one.

The spectroscopic evolution of all II-P SNe is rather homogeneous, showing hydrogen and metal lines with P-Cygni profiles having typical widths ranging from about 15 000 to 3000 km s^{-1} during the photospheric phase.

A common feature of most light curves of Type II SNe is the linear tail, produced by the radioactive decay of ^{56}Co into ^{56}Fe (0.98 mag/100^d). While in some cases condensation of dust grains in the ejecta and ejecta–CSM interaction phenomena may affect the late-time evolution, there is nevertheless general agreement that the radioactive tail of a 'typical' CC-SN is powered by $\sim$0.06–0.10 $M_\odot$ of ^{56}Ni (see e.g. Turatto et al. 1990; Sollerman 2002).

However, in recent years, systematic observations of non-interacting SNe in the nebular phase have shown that CC-SNe are also heterogeneous at late stages and the following more complex picture has emerged.

(i) A few CC-SNe, sometimes called *hypernovae* (Iwamoto et al. 1998), show evidence of exceptionally large Ni masses, 0.3–0.9 $M_\odot$ (Sollerman et al. 2000; Patat et al. 2001; see, however, Höflich, Wheeler & Wang 1999) who find $\sim$0.2 $M_\odot$ of ejected ^{56}Ni assuming asymmetric explosions. In addition, some otherwise 'normal' II-P SNe have produced unusually bright radioactive tails, again implying large amounts of ^{56}Ni – see e.g. SN 1992am ($\sim$0.3 $M_\odot$) (Schmidt et al. 1994).

(ii) In most CC-SNe the late-time luminosity is produced by 0.06–0.10 $M_\odot$ of ^{56}Ni, see e.g. SN 1987A (II pec; Catchpole et al. 1987; Menzies et al. 1987; Catchpole et al. 1988; Whitelock et al. 1988; Catchpole et al. 1989; Whitelock et al. 1989), SN 1988A (II-P; Ruiz-Lapuente et al. 1990; Benetti, Cappellaro & Turatto 1991; Turatto et al. 1993), SN 1993J (IIb; see e.g. Barbon et al. 1995) and SN 1994I (Ic; Young, Baron & Branch 1995; Richmond et al. 1996, and references therein).

(iii) A few events exhibit a somewhat lower late-time luminosity, such as SN 1991G (Blanton et al. 1995), SN 1992ba (Hamuy 2003) and SN 1999gi (Leonard et al. 2002b; Hamuy 2003). This may be attributable to the ejection of reduced amounts of ^{56}Ni (0.015–0.04 $M_\odot$). Conversely, it could be that the luminosity of these SNe is greater, but the distances and/or the effects of interstellar absorption have been underestimated. This might be the case of SN 1999em (Baron et al. 2000; Leonard et al. 2002a; Pooley et al. 2002; Hamuy et al. 2001; Elmhamdi et al. 2003) for which recent Cepheid distance measurements Leonard et al. (2003) suggest that the host galaxy distance was previously underestimated and, consequently, the SN luminosity is probably higher. The Type II plateau supernova SN 1994W (Sollerman, Cumming & Lundqvist 1998), while having an exceptionally high luminosity during the photospheric era, was also particularly faint at late times with an ejected ^{56}Ni mass below 0.015 $M_\odot$, depending inversely on the assumed contribution to the luminosity of an ejecta–CSM interaction.

(iv) Finally, there is a small group of events having very-low late-time luminosities. The prototype is SN 1997D (Turatto et al. 1998). As demonstrated in this paper, the SNe of this group are also exceptionally faint at early-times. The other SNe in this category that we study here are SN 1994N (Turatto, Gouiffes & Leibundgut 1994), SN 1999br (King 1999), SN 1999eu (Nakano & Aoki 1999) and SN 2001dc (Hurst et al. 2001). As we shall see, the late-time light curves of this group require very small amounts of ^{56}Ni, at least one order of magnitude smaller than in SN 1987A.

In a companion paper (Zampieri et al. 2003) we performed an analysis of the data of SN 1997D and SN 1999br, deriving information about the nature of the progenitor stars and the explosion energies. The early observations of SN 1999br allowed us to constrain the models discussed in previous papers (Turatto et al. 1998; Chugai & Utrobin 2000). We found that these explosions are under-energetic with respect to a typical Type II SN and that the inferred mass of the ejecta is large ($M_{\rm ej} \geqslant$ 14–20 $M_\odot$).

In this paper we present the spectroscopic and photometric observations of the very-low-luminosity SNe 1999br, 1999eu, 1994N and 2001dc. Together with the SN 1997D data (Turatto et al. 1998; Benetti et al. 2001) these make up almost all that is available for this group of SNe. The plan of the paper is as follows. In Section 2 we describe the SNe and their parent galaxies. In particular, we estimate distances, crucial for the derivation of the luminosity and, in turn, of the ^{56}Ni mass. The observations are summarized in Section 3. In Section 4 we present photometric data and in Section 5 we analyse light and colour curves, focusing on the common properties of this group of SNe and making comparisons with the prototype SN 1997D. In Section 6 spectroscopic observations are presented. In Section 7 we discuss the data with particular focus on the nature of the progenitors. Section 8 is devoted to an estimate of the frequency of these low-luminosity events. A short summary follows in Section 9.

Throughout this paper we adopt $H_0 = 65$ km s^{-1} Mpc^{-1}. In all the images, North is up, East is to the left and the numbers label stars of the local calibration sequence.

2 THE SNE AND THEIR HOST GALAXIES

In Table 1 we summarize the main observational data for our sample of SNe and their host galaxies. For completeness, we show also the parameters for SN 1997D in this table.

(i) SN 1999br was discovered by King (1999) in the course of the Lick Observatory Supernova Search on 1999 April 12.4 UT, and confirmed the following day, when its magnitude was about 17.5. It was located at $\alpha = 13^{\rm h}00^{\rm m}41\overset{\rm s}{.}8, \delta = +02^\circ29'45\overset{''}{.}8$ (equinox 2000.0), about 40 arcsec East and 19 arcsec South from the nucleus of NGC 4900 and near a bright foreground star (12.5 arcsec West and 15.6 arcsec South) of eleventh magnitude (see Fig. 1). SN 1999br is the first 1997D-like event discovered a few days after the explosion. There was no evidence of the SN on frames taken on 1999 March 27.4 UT (limiting magnitude 18.5) and on 1999 April 4.4 (limiting magnitude 17; Li 1999, see also Fig. 2). The SN was classified as a peculiar, faint Type II event (Filippenko, Stern & Reuland 1999; Garnavich et al. 1999a). Patat et al. (1999) pointed out the similarity with SN 1994N at a comparable phase and suggested that SN 1999br had produced a very-low amount of ^{56}Ni.

The host galaxy (Fig. 1) of SN 1999br, NGC 4900, is a well studied SB(rs)c galaxy lying in the direction of the Virgo Cluster. Different estimates of the distance have been published for this galaxy (Bottinelli et al. 1985; Kraan-Korteweg 1986; Ekholm et al. 2000; Fouquè et al. 2000; Freedman et al. 2001). The recession velocity of NGC 4900 corrected for the Local Group infall on to the Virgo Cluster (from the LEDA catalogue) is $v_{\rm vir} = 1013$ km s^{-1}. This is close to the average value for the group, dominated by NGC 4517, to which NGC 4900 belongs ($\langle v_{\rm vir} \rangle = 1125$ km s^{-1}, Giuricin et al. 2000), resulting in a distance modulus of $\mu = 31.19$. This is the final value adopted for SN 1999br (see Table 1).

Table 1. Main observational data for the low-luminosity Type II SNe and their host galaxies.

SNe Data	1997D		1999br		1999eu		1994N		2001dc	
α (J2000.0)	$04^h11^m01\overset{s}{.}00$	•	$13^h00^m41\overset{s}{.}80$	△	$02^h46^m20\overset{s}{.}79$	◇	$10^h29^m46\overset{s}{.}8$	▽	$14^h51^m16\overset{s}{.}15$	∗
δ (J2000.0)	$-56°29'56\overset{''}{.}0$	•	$+02°29'45\overset{''}{.}8$	△	$-30°19'06\overset{''}{.}1$	◇	$+13°01'14''$	▽	$+58°59'02.8$	∗
Offset SN–gal.nucleus	11″E, 43″S	•	40″E, 19″S	△	23″E, 157″S	◇	$1\overset{''}{.}8$E, $9\overset{''}{.}8$N	▽	26″W, 28″N	∗
Discovery date (UT)	1997 Jan 14.15	•	1999 Apr 12.4	△	1999 Nov 5	◇	1994 May 10.0	▽	2001 May 30.96	∗
Discovery Julian date	245 0462.65	•	245 1280.9	△	245 1487.5	◇	244 9482.5	▽	245 2060.46	∗
Explosion epoch (JD)	245 0361	×	245 1278	×	245 1394	×	244 9451	×	245 2047	×
Discovery magnitude	16.3 (Jan 15.05)	•	$m = 17.5$	△	$m = 17.3$	◇	$R = 17.5$	▽	$m = 18.5$	∗
V(max)	⩽19.8	×	⩽16.8	◇	17.5	×	⩽17.3	×	⩽18.5	×
Total extinction $A_{B,tot}$	0.089	×	0.102	×	0.113	×	0.169	×	1.7	×
Host galaxies data	NGC 1536		NGC 4900		NGC 1097		UGC 5695		NGC 5777	
α (J2000.0)	$04^h10^m59\overset{s}{.}86$	†	$13^h00^m39\overset{s}{.}13$	†	$02^h46^m19\overset{s}{.}06$	†	$10^h29^m46\overset{s}{.}8$	†	$14^h51^m18\overset{s}{.}55$	†
δ (J2000.0)	$-56°28'49\overset{''}{.}6$	†	$+02°30'05\overset{''}{.}3$	†	$-30°16'29\overset{''}{.}7$	†	$+13°01'05\overset{''}{.}5$	†	$+58°58'41\overset{''}{.}4$	†
Morph. Type	SB(s)c pec	†	SB(rs)c	†	SBbSy1	†	S?	†	Sbc	†
B magnitude	13.15	†	11.90	†	10.23	†	14.66	†	14.11	†
Galactic extinction A_B	0.092	⊗	0.102	⊗	0.113	⊗	0.169	⊗	0.046	⊗
Diameters	$2\overset{'}{.}0 \times 1\overset{'}{.}4$	†	$2\overset{'}{.}2 \times 2\overset{'}{.}1$	†	$9\overset{'}{.}3 \times 6\overset{'}{.}3$	†	$1\overset{'}{.}3 \times 0\overset{'}{.}5$	†	$3\overset{'}{.}38 \times 0\overset{'}{.}45$	†
v_{hel} (km s^{-1})	1461	⋆	968	⋆	1273	⋆	2940	⋆	2140	⋆
μ ($H_0 = 65$ km s^{-1} Mpc^{-1})	31.29	×	31.19	○	31.08	×	33.34	×	32.85	×

⋆ LEDA (http://leda.univ-lyon1.fr/search.html); † NED (http://nedwww.ipac.caltech.edu/index.html); △ King (1999); ⊗ Schlegel et al. (1998); ◇ Nakano & Aoki (1999); ▽ Turatto et al. (1994); ∗ Hurst et al. (2001); ○ Giuricin et al. (2000); • de Mello & Benetti (1997); ◇ Benetti et al. (2001); × this paper.

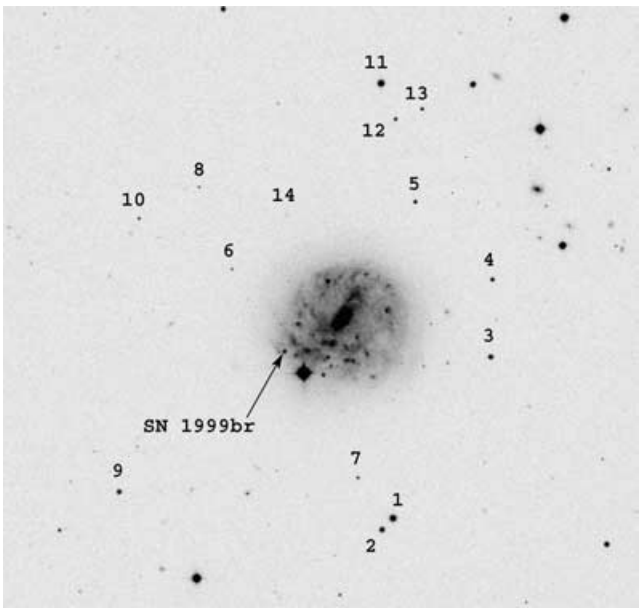

Figure 1. *V*-band image of SN 1999br and the host galaxy NGC 4900 (image obtained on 1999 July 6 with ESO-Danish 1.54-m telescope + DFOSC).

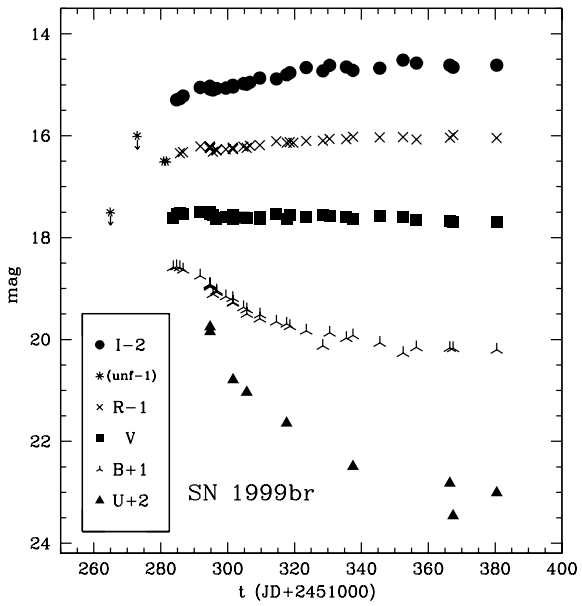

Figure 2. *UBVRI* light curves of SN 1999br showing its extended plateau. Two prediscovery limits (IAU Circ. 7143), unfiltered measurements, are also shown placed to correspond with the *R*-magnitude scale (IAU Circ. 7141). Photometry from Hamuy et al. (in preparation) is also shown.

For the galactic extinction, we adopt $A_B = 0.102$ (Schlegel, Finkbeiner & Davis 1998); no sign of internal extinction (e.g. lack of narrow interstellar Na I D lines) is present in the spectra of SN 1999br, which is not unexpected given the peripheral location of the SN in NGC 4900.

(ii) SN 1999eu was discovered by Nakano & Aoki (1999) with a 0.40-m reflector on 1999 November 5 and confirmed the following day. The SN was located at $\alpha = 02^h46^m20\overset{s}{.}79$, $\delta = -30°19'06\overset{''}{.}1$ (equinox 2000.0), 23 arcsec East, 157 arcsec South from the nucleus of NGC 1097, lying on an arm with a relatively flat background structure (see Fig. 3). Garnavich et al. (1999b) classified SN 1999eu as a peculiar Type II SN, with a spectrum characterized by several narrow P-Cygni lines and a typical velocity of ∼1500 km s^{-1} (from the minimum of Ba II λ6142). Garnavich et al. concluded that SN 1999eu was an under-luminous Type II event powered by the ejection of an extremely small amount of ^{56}Ni.

The host galaxy, NGC 1097, is a peculiar barred spiral listed in Arp's Catalogue (1966). Sersic (1973) noted that the galaxy nucleus was morphologically peculiar with a central condensation, surrounded by an annulus of hotspots, almost uniformly and

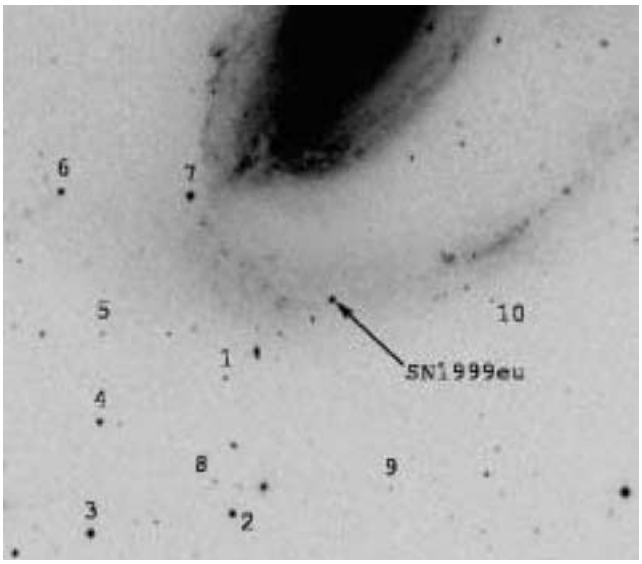

Figure 3. SN 1999eu in NGC 1097 (*R*-band image with ESO-Danish 1.54-m telescope + DFOSC).

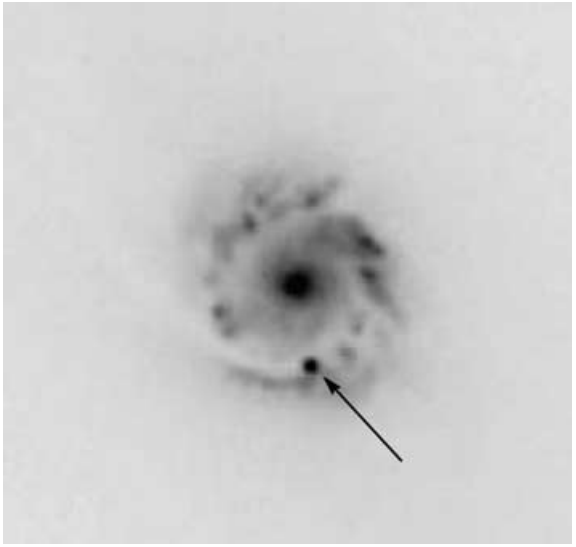

Figure 4. The annulus of H II regions and hotspots surrounding the nucleus of NGC 1097, possibly a region of intense star formation. The frame was taken on 1992 October 16 with NTT + EMMI (filter R) and includes the Type II SN 1992bd, indicated by an arrow. NGC 1097 also hosted SN 1999eu, studied in this paper, as well as the Type II SN 2003B.

symmetrically distributed (Fig. 4). Wolstencroft, Tully & Perley (1984) found that this structure was composed of H II regions emitting at radio wavelengths. The observations suggest that a burst of star formation is taking place in the ring. This is supported also by the discovery of the core-collapsed SN 1992bd (Smith et al. 1992) in this region (Fig. 4). The nucleus of the galaxy is a compact radio source and shows the emission line spectrum of a type 1 Seyfert galaxy (Storchi-Bergmann et al. 1997). We also note that the Type II SN 2003B was discovered in a peripheral region of the galaxy, close to the nearby small elliptical companion NGC 1097A (Evans & Quirk 2003).

Contrary to what is sometimes claimed, NGC 1097 membership of the Fornax cluster is uncertain (Giovanelli et al. 1997). The galaxy

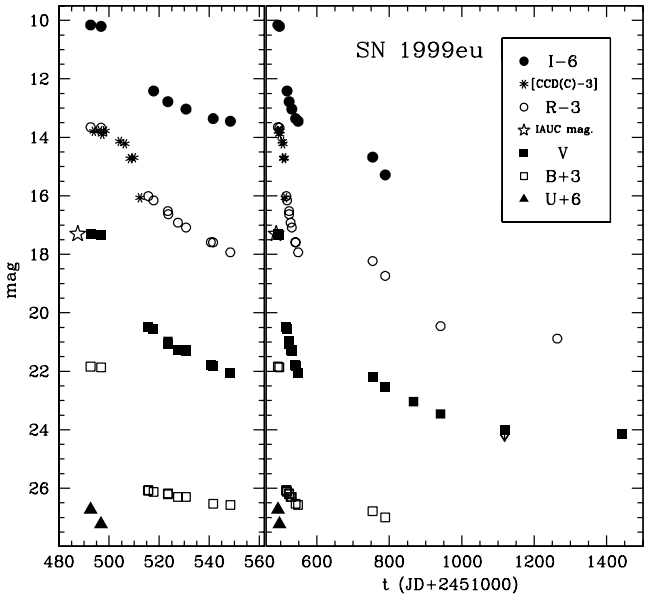

Figure 5. *BVRI* light curves of SN 1999eu. Left: enlargement of the first two months. Right: complete light curves. Two points in the *U* band are also reported. The star (plotted with respect to the *V* magnitude scale) refers to the discovery unfiltered magnitude (IAUC 7304 Nakano & Aoki 1999). The asterisks are taken from the web sites http://aude.geoman.net/observation/SN/infc99eu.htm and VSNET (http://www.kusastro.kyoto-u.ac.jp/vsnet/), and are plotted with respect to the *R*-magnitude scale.

velocity is close to the average value of the group NOG 179, to which NGC 1097 belongs (Giuricin et al. 2000). The recession velocity corrected for Virgo infall was derived from the LEDA catalogue, which yields $v_{\rm vir} = 1069$ km s^{-1}. The resulting distance modulus is $\mu = 31.08$ (Table 1).

For the galactic extinction, we adopt $A_B = 0.113$ (Schlegel et al. 1998). There is no spectroscopic evidence for strong extinction in the host galaxy.

(iii) SN 1994N was serendipitously discovered by Turatto et al. (1994) with the ESO 3.6-m telescope during an observation of the Type IIn SN1993N, which exploded the year before in the same galaxy (Mueller et al. 1993). The new SN was located at $\alpha = 10^{\rm h}29^{\rm m}46\overset{\rm s}{.}8$, $\delta = +13^\circ01'14''$ (equinox 2000.0), 1.8 arcsec East and 9.8 arcsec North from the nucleus of the spiral galaxy UGC 5695, not far (8.5 arcsec East) from SN 1993N.

Little information on UGC 5695 is available. It is a member of a small group of galaxies, LGG 207, which has a mean heliocentric velocity of 2856 km s^{-1} (Garcia 1993), slightly larger than that of the galaxy itself. Taking LEDA's heliocentric velocity of UGC 5695 corrected for Virgo infall and for the peculiar motion inside the group (+48 km s^{-1}), we derive a distance modulus $\mu = 33.34$.

Because evidence of strong internal extinction is missing from our spectra, we have applied only the galactic extinction correction $A_B = 0.169$ (Schlegel et al. 1998).

(iv) Armstrong (2001) discovered SN 2001dc at $\alpha = 14^{\rm h}51^{\rm m}16\overset{\rm s}{.}15$ and $\delta = +58^\circ59'02\overset{''}{.}8$ (equinox 2000.0), 26 arcsec West and 28 arcsec North of the centre of NGC 5777 (see Fig. 8, later). A prediscovery upper limit indicates that SN 2001dc was discovered only a few days after explosion. From early photometric monitoring, Hurst et al. (2001) noted that this event could be classified as a II-P SN and concluded that the event was unusually

under-energetic, with an absolute magnitude very low compared with normal II-P SNe.

The host galaxy NGC 5777 is an edge-on Sbc galaxy, crossed by a spectacular equatorial dust lane (Bottinelli et al. 1990). From LEDA we derive a heliocentric velocity of 2140 km s^{-1} and, after correcting for Virgo infall, $v_{\rm vir} \approx 2419$ km s^{-1}, $\mu = 32.85$ (see Table 1).

The galactic extinction is $A_B = 0.046$ (Schlegel et al. 1998). The position of the SN, not far from the nucleus and projected on to a background rich in gas and dust, leads us to suspect the presence of some internal extinction. We shall discuss this point in Section 5.

3 SUMMARY OF THE OBSERVATIONS

Our observations of SNe 1999br, 1999eu, 1994N and 2001dc were obtained with the ESO, CTIO, ING, TNG and Asiago telescopes. Images and spectra were reduced using standard IRAF or FIGARO procedures. The photometric data are presented in Section 4. The magnitudes of the SNe were obtained using either PSF fitting or template subtraction techniques, depending on the background complexity and the availability of suitable template images.

The journal of spectroscopic observations is reported in Table 2. The spectra of SNe 1999eu, 1994N and 2001dc are presented here for the first time. All the spectra were flux calibrated using standard stars (selected from Hamuy et al. 1992, 1994; Stone 1977; Stone & Baldwin 1983; Baldwin & Stone 1984) observed during the same nights.

The photometric and spectroscopic observations of SN 1999br provide good coverage of the plateau phase, but only sparse data are available in the nebular phase. In particular, no post-plateau spectra are available. The discovery epoch of SN 1999eu was probably long after the explosion, at the end of the plateau, although it was well observed both photometrically and spectroscopically at late epochs. The data for SN 1994N are sparse, although they do span a period of about 22 months. The photometric coverage of SN 2001dc began about one month after discovery. Because of its faintness, it was not possible to observe it long after the end of the plateau. Three spectra were also obtained, all during the plateau phase. Clearly, the temporal coverage of individual low-luminosity SNe is incomplete and erratic. However, we shall argue that these events form a fairly homogeneous group and so, taken together, they provide a reasonably complete picture of the photometric and spectroscopic evolution of this type of supernova.

4 LIGHT CURVES

4.1 SN 1999br

The Tololo Group performed an intensive follow-up of SN 1999br during the plateau phase with the CTIO and ESO telescopes (Hamuy 2003; Hamuy et al., in preparation). We also observed this SN using the ESO telescopes and TNG. Our optical photometry in the *UBVRI* bands is shown in Table 3. The SN magnitudes were calibrated by means of a local sequence (Hamuy et al., in preparation) after comparison with Landolt standard stars (Landolt 1992). The photometric measurements of SN 1999br were performed using the template subtraction technique. The template images were obtained on 2000 April 2 (NTT + EMMI) and 2001 February 1 (ESO 3.6 m + EFOSC2). The errors were computed by placing some artificial stars (having the same magnitude as the SN) at positions close to the SN, and hence estimating the deviations in the measured magnitudes.

The first season *UBVRI* light curves are shown in Fig. 2 which also includes the data from Hamuy et al. (in preparation). A pre-discovery limit from IAU Circ. 7143 allows us to fix the explosion epoch between JD = 245 1264.9 and 245 1280.9. Another limit obtained on JD = 245 1272.9 is less stringent. Hereafter we adopt as the explosion epoch JD = 245 1278±3, which is compatible with the assumptions of Zampieri et al. (2003). While the *U* and *B* band light curves decline monotonically after discovery (the slope of the *B* band light curve is 3.66 mag/100^d during the first 40 d and

Table 2. Journal of spectroscopic observations (JD +240 0000).

Date	JD	Phase	Instrument	Range (Å)	Resolution (Å)
			SN 1994N		
10/05/94	49482.54	31.5	3.6^m+EFOSC1	3700–9850	13, 17
14/05/94	49486.56	35.6	2.2^m+EFOSC2	4500–7150	11
05/06/94	49508.53	57.5	3.6^m+EFOSC1	3700–6900	18
30/01/95	49747.80	296.8	NTT+EMMI	3850–8950	9
			SN 1999br		
23/04/99[a]	51291.73	13.7	LCO100	3700–9300	5
26/04/99[a]	51294.64	16.6	1.54^m+DFOSC	3500–9800	14, 19
29/04/99[a]	51297.68	19.7	NTT+EMMI	3350–10250	7, 6
03/05/99[a]	51301.64	23.6	NTT+EMMI	3300–10100	7, 6
11/05/99[a]	51309.69	31.7	1.54^m+DFOSC	3700–10100	14, 19
19/05/99[a]	51317.68	39.7	NTT+EMMI	3400–10100	7, 6
21/05/99	51320.02	42.0	3.6^m+EFOSC2	3350–10250	14, 17
20/07/99	51380.45	102.5	1.54^m+DFOSC	3400–9050	12
			SN 1999eu		
10/11/99	51492.64	98.6	1.54^m+DFOSC	3450–9050	11
14/11/99	51496.81	102.8	3.6^m+EFOSC2	3400–7500	17
05/12/99	51517.74	123.7	3.6^m+EFOSC2	3350–10250	14, 17
18/12/99	51530.71	136.7	3.6^m+EFOSC2	3400–7450	17
			SN 2001dc		
10/07/01	52101.48	54.5	INT+IDS	4850–9600	17
16/08/01	52138.44	91.4	TNG+DOLORES	3300–8000	15
24/08/01	52146.43	99.4	WHT+ISIS	3750–9950	14

[a]Hamuy & Phillips, private communication.

Table 3. Photometry of SN 1999br (JD +240 0000).

Date	JD	*U*	*B*	*V*	*R*	*I*	Instrument
21/05/99	51319.65	–	–	–	17.14 (0.04)	–	1
07/06/99	51337.50	20.49 (0.29)	18.92 (0.01)	17.63 (0.01)	17.02 (0.01)	16.72 (0.01)	2
06/07/99	51366.47	20.82 (0.37)	19.17 (0.09)	17.68 (0.01)	17.04 (0.01)	16.62 (0.01)	3
07/07/99	51367.45	21.46 (0.55)	19.18 (0.03)	17.69 (0.04)	16.98 (0.02)	16.66 (0.01)	2
20/07/99	51380.48	21.01 (0.31)	19.20 (0.03)	17.69 (0.01)	17.04 (0.02)	16.62 (0.01)	3
02/04/00	51636.59	–	–	22.60 (0.15)	–	21.18 (0.24)	4[a]
09/04/00	51643.69	–	–	22.68 (0.08)	–	–	4[a]
02/05/00	51666.67	–	–	–	21.98 (0.05)	–	4[a]
01/02/01	51941.87	–	–	$\geqslant$24.4	$\geqslant$24.6	–	1
26/07/01	52117.50	–	–	$\geqslant$25.2	$\geqslant$24.8	–	5

Notes: 1 = ESO 3.6-m + EFOSC2; 2 = TNG + OIG. 3 = Danish 1.54-m + DFOSC; 4 = NTT + EMMI; 5 = ESO VLT + FORS1. [a]Hamuy & Phillips, private communication.

Table 4. Optical and infrared photometry of SN 1999eu (JD +240 0000).

Date	JD	*U*	*B*	*V*	*R*	*I*	*J*	*H*	*Ks*	Ins.
10/11/99	51492.64	20.73 (0.08)	18.84 (0.01)	17.29 (0.01)	16.65 (0.01)	16.16 (0.01)	–	–	–	1
12/11/99	51494.69	–	–	–	–	–	15.81 (0.01)	15.61 (0.01)	15.50 (0.02)	7
13/11/99	51496.79	21.23 (0.06)	18.87 (0.01)	17.34 (0.01)	16.67 (0.01)	16.21 (0.01)	–	–	–	2
02/12/99	51515.66	–	23.06 (0.13)	20.50 (0.13)	19.01 (0.04)	–	–	–	–	4
02/12/99	51515.66	–	23.09 (0.23)	–	–	–	–	–	–	4
04/12/99	51517.76	–	23.13 (0.33)	20.56 (0.05)	19.16 (0.05)	18.41 (0.18)	–	–	–	2
10/12/99	51523.48	–	23.21 (0.19)	20.98 (0.07)	19.52 (0.02)	18.78 (0.12)	–	–	–	5
11/12/99	51523.64	–	23.17 (0.17)	21.05 (0.09)	19.63 (0.02)	–	–	–	–	4
15/12/99	51527.50	–	23.29 (0.23)	21.27 (0.06)	19.92 (0.02)	–	–	–	–	5
18/12/99	51530.73	–	23.30 (0.39)	21.28 (0.12)	20.08 (0.04)	19.04 (0.03)	–	–	–	2
18/12/99	51530.73	–	–	21.31 (0.13)	–	–	–	–	–	2
28/12/99	51540.65	–	–	21.80 (0.61)	20.59 (0.21)	–	–	–	–	4
28/12/99	51540.65	–	$\geqslant$22.68 (0.28)	–	–	–	–	–	–	4
29/12/99	51541.53	–	23.53 (0.17)	21.81 (0.12)	20.59 (0.02)	19.36 (0.01)	–	–	–	1
04/01/00	51548.39	–	23.58 (0.18)	22.05 (0.08)	20.93 (0.03)	19.45 (0.19)	–	–	–	5
27/07/00	51753.92	–	23.78 (0.17)	22.20 (0.10)	21.23 (0.08)	20.68 (0.03)	–	–	–	3
31/08/00	51788.85	–	24.00 (0.40)	22.54 (0.25)	21.74 (0.16)	21.28 (0.11)	–	–	–	2
10/11/00	51858.73	–	–	–	–	–	21.93 (0.43)	20.62 (0.34)	20.50 (0.30)	7
19/11/00	51866.71	–	–	23.04 (0.10)	–	–	–	–	–	1
01/02/01	51941.54	–	–	23.46 (0.13)	23.46 (0.10)	–	–	–	–	2
27/07/01	52117.87	–	–	$\geqslant$24.0	–	–	–	–	–	6
20/12/01	52263.68	–	–	–	23.88 (0.17)	–	–	–	–	6
23/06/02	52441.87	–	–	24.15 (0.40)	–	–	–	–	–	6

Notes: 1 = ESO Dan 1.54-m + DFOSC; 2 = ESO 3.6-m + EFOSC2; 3 = ESO NTT + EMMI; 4 = ESO 2.2m + WFI + chip7, 5 = TNG + OIG; 6 = VLT + FORS1; 7 = NTT + SOFI.

0.61 mag/100^d later), the *V*-band light curve shows a plateau of duration at least 100 d. Between about days 30 and 100, the slope is $\gamma_V \approx$ 0.20 mag/100^d. The *R*- and *I*-band magnitudes increase with time up to the last data point at ∼100 d. During the era 30–100 d, the slopes are, respectively, $\gamma_R \approx -0.18$ and $\gamma_I \approx -0.25$ mag/100^d. This evolution is typical of a Type II SN during the plateau phase (Popov 1992). Unfortunately, no measurements are available between 1999 July 20, and 2001 February 1, and so the precise length of the plateau phase is undetermined. Only a few measurements or upper limits (see e.g. Fig. 12, later) are available during the radioactive decay epoch, but they are of special interest owing to their role in the determination of the ^{56}Ni mass.

4.2 SN 1999eu

Our photometry, covering a period of ∼950 d, is shown in Table 4. Lacking a reference image, the SN magnitudes were obtained using a PSF-fitting technique. The errors were estimated using artificial stars, as described above. In Table 5 we give the magnitudes of the local sequence stars (see Fig. 3). SN 1999eu was observed twice in the IR with NTT + SOFI. The *JHK* magnitudes are also reported in Table 4. From these observations alone it is impossible to reach a definitive conclusion on the evolution of the light curve in the IR bands, but they can help in evaluating the bolometric correction at selected epochs. Comparison with the IR light curves of CC-SNe compiled by Mattila & Meikle (2001) places the earlier *JHK* photometry of SN 1999eu about 1.2 magnitudes fainter than the average values for 'ordinary' CC-SNe for this phase (∼100 d), and similar in magnitude to SN 1982R. We stress that the last very faint detection could also be due to IR background emission.

About one week after discovery, the light curves underwent an abrupt fall in brightness (especially at shorter wavelength bands). About three weeks post-discovery, a slower decline took over. This was observed to continue until the SN was lost behind the Sun about

Table 5. Magnitudes of the sequence stars in the field of NGC 1097. The numbers in brackets are the rms of the available measurements. If no error is reported, only a single estimate is available. We estimated the errors in *J*, *H*, *Ks* as the deviation from the average of two available measurements.

Star	*U*	*B*	*V*	*R*	*I*	*J*	*H*	*Ks*
1	21.78 (–)	21.13 (0.01)	19.95 (0.02)	19.20 (0.01)	18.44 (0.01)	17.31 (0.10)	16.97 (0.01)	16.94 (0.01)
2	18.14 (0.01)	17.68 (0.02)	16.77 (0.01)	16.19 (0.03)	15.72 (0.02)	15.16 (0.02)	14.63 (0.02)	14.67 (0.02)
3	19.13 (–)	18.41 (0.01)	16.64 (0.01)	15.56 (0.03)	14.01 (0.06)	–	–	–
4	20.24 (–)	19.26 (0.02)	18.00 (0.01)	17.14 (0.01)	16.41 (0.01)	15.55 (0.10)	14.91 (0.04)	14.84 (0.03)
5	–	23.31 (0.01)	21.43 (0.01)	20.41 (0.02)	19.40 (0.02)	18.12 (0.06)	17.35 (0.12)	16.93 (0.05)
6	19.45 (0.01)	18.49 (0.02)	17.58 (0.02)	16.94 (0.03)	16.38 (0.01)	–	–	–
7	17.23 (0.03)	16.95 (0.03)	16.23 (0.01)	15.77 (0.03)	15.38 (0.01)	14.90 (0.01)	14.51 (0.02)	14.51 (0.06)
8	22.85: (–)	23.04 (0.05)	21.22 (0.06)	20.45 (0.04)	20.08 (0.01)	18.86 (0.09)	18.03 (0.02)	17.78 (0.11)
9	21.06 (–)	21.26 (0.02)	20.63 (0.01)	20.23 (0.02)	19.80 (0.03)	19.34 (0.02)	–	–
10	22.29 (–)	21.57 (0.02)	20.59 (0.03)	19.97 (0.02)	19.52 (0.06)	18.61 (0.11)	–	17.99 (0.03)

Table 6. Slopes of the light curves of SN 1999eu in the *B*-, *V*-, *R*- and *I*-bands (in mag/100^d). The phase is with respect to the day of explosion (JD = 245 1394).

Band	95–125	120–160	150–365	355–550	540–1050
γ_B	19.77	1.60	0.11	0.61	–
γ_V	14.31	4.78	0.07	0.66	0.14
γ_R	10.05	5.68	0.14	1.17	0.13
γ_I	9.48	3.30	0.60	1.74	–

nine weeks post-discovery. When the SN was recovered ∼seven months later, it was only marginally fainter. The second season light curves (especially the bolometric curve, cf. Section 5) follow roughly the ^{56}Co decay exponential decline rate. The slopes in the *B*-, *V*-, *R*- and *I*-passbands are given in Table 6. The last two very faint detections possibly indicate a flattening in the light curve, but we cannot exclude strong background contamination. By analogy with the other faint SNe (see Section 6) we believe that SN 1999eu was discovered near the end of the plateau phase, about three months after the explosion. Unfortunately, useful constraints on the length of the plateau phase are not available since the latest prediscovery image was taken about one year before discovery (Nakano & Aoki 1999).

4.3 SN 1994N

The photometry of SN 1994N is sparse (see Table 7). It was obtained using ESO-La Silla telescopes, often under poor weather conditions. The late-time photometry was performed using the template subtraction technique. Again, the errors were estimated using artificial stars. As standard stars we adopted the local sequence in the field of UGC 5695 calibrated during some photometric nights in 1993 (during the follow-up of SN 1993N). The magnitudes of the sequence stars (Fig. 6) are given in Table 8. The light curve shows that this SN was discovered during the plateau phase. The prediscovery upper limits constrain the explosion epoch to no earlier than about seven weeks before discovery (see Fig. 7). We measure the slope during the plateau and find, respectively, $\gamma_V \approx 0$ and $\gamma_R \approx -0.3$ mag/100^d, although, given that there are only a few points in the *V*- and *R*-band light curves, we regard this measurement as tentative. At late times, the observations indicate $\gamma_V \approx 1$ mag/100^d, although the photometric errors are sometimes quite large.

Table 8. Magnitudes of the sequence stars in the field of UGC 5695. The numbers in brackets are the rms of the available measurements. Uncalibrated *U* and *I* magnitudes of sequence stars obtained on 1994 May 13 are also reported.

Star	*U*	*B*	*V*	*R*	*I*
2	–	–	14.54 (0.01)	14.16 (0.01)	–
3	–	–	14.93 (0.03)	14.49 (0.01)	–
4	18.19 (–)	18.21 (0.02)	17.47 (0.01)	17.04 (0.02)	16.77 (–)
5	17.33 (–)	17.60 (0.02)	16.98 (0.01)	16.67 (0.01)	16.40 (–)
6	–	20.06 (0.02)	18.85 (0.01)	18.21 (0.01)	17.74 (–)
7	–	–	20.24 (0.01)	18.91 (0.04)	17.32 (–)

4.4 SN 2001dc

Our photometry measurements of SN 2001dc, lacking template images, were obtained using the PSF fitting technique. The magnitudes

Table 7. Photometry of SN 1994N (JD +240 0000).

Date	JD	*U*	*B*	*V*	*R*	*I*	Instrument
17/03/94	49428.5	–	–	⩾22.50	⩾21.20	–	1
09/05/94	49482.48	–	19.44 (0.04)	18.50 (0.02)	18.12 (0.02)	–	2
13/05/94	49486.48	20.44 (0.25)	19.48 (0.01)	18.55 (0.01)	18.14 (0.01)	17.95 (0.02)	3
05/06/94	49508.52	–	–	18.52 (0.05)	18.05 (0.04)	–	2
31/12/94	49717.76	–	–	–	21.90 (0.15)	–	3
10/01/95	49727.80	–	–	22.77 (0.03)	22.03 (0.04)	–	4
30/01/95	49747.74	–	–	–	22.22 (0.08)	–	1
16/03/96	50158.5	–	⩾22.23	⩾22.95	⩾22.07	–	2

Notes: 1 = NTT + EMMI; 2 ESO 3.6-m + EFOSC1; 3 = ESO 2.2-m + EFOSC2; 4 = NTT + SUSI.

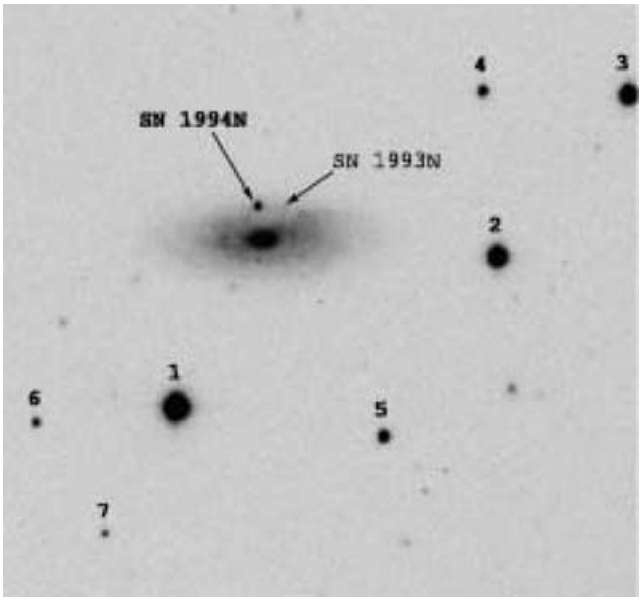

Figure 6. SN 1994N and the Type IIn SN 1993N in UGC 5695 (*R*-band image taken with the ESO 3.6-m telescope + EFOSC1 on 1994 May 9).

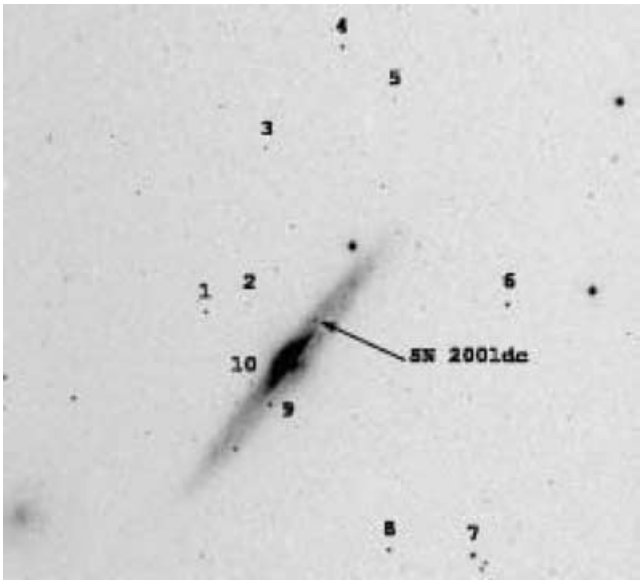

Figure 8. SN 2001dc in NGC 5777 (*R*-band image taken with JKT + IAG ccd on 2001 July 13).

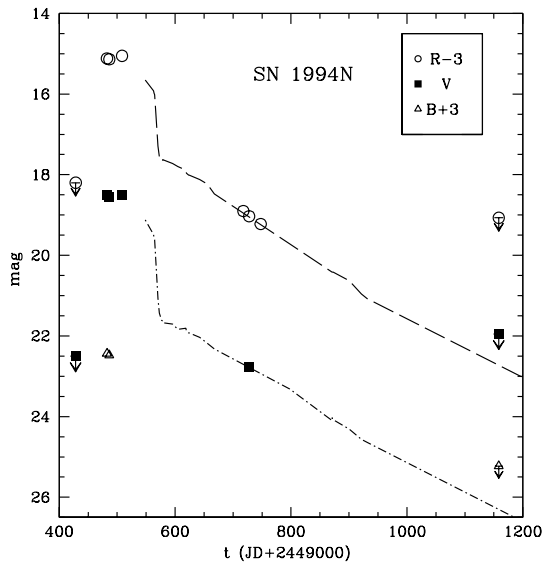

Figure 7. *B*-, *V*- and *R*-band light curves of SN 1994N. The dashed lines represent the *V*- and *R*-band light curves of SN 1997D shifted in magnitude and in time to match the points of SN 1994N, plotted to guide the eye.

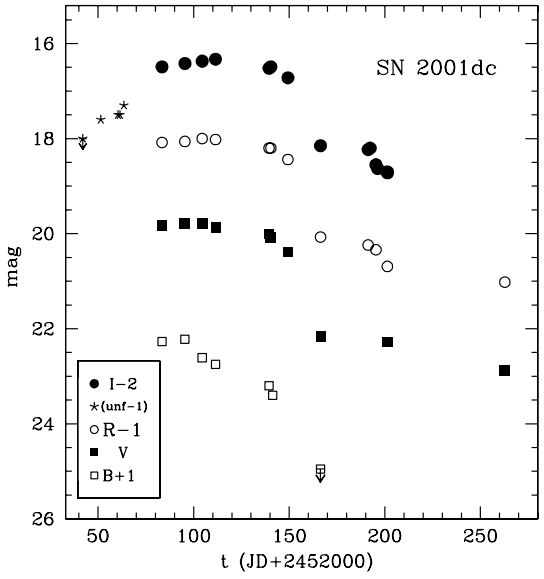

Figure 9. *BVRI* light curves of SN 2001dc. The unfiltered prediscovery limit and magnitudes (asterisks) are shown with respect to the *R*-magnitude scale (Hurst et al. 2001). The magnitude at phases later than ∼100 d are affected by large errors.

are reported in Table 9. The large errors at late times (estimated with the artificial stars method) are caused by the complex background upon which the SN is projected. Table 10 gives the magnitudes of the local sequence stars (Fig. 8). The light curves are shown in Fig. 9. In the following, we adopt 2001 May 17 (JD = 245 2047 ± 5) as the explosion epoch, this being intermediate between the upper limit of May 12 and the first (prediscovery) detection on May 21.98.

The light curve shows a plateau persisting to 90–100 d post explosion. The slope of the light curves for three representative epochs are reported in Table 11. Despite the large errors due to the faintness of the SN and its position, the slopes in *V* and *R* during ∼115–220 d are rather close to the luminosity decline rate of ^{56}Co.

5 COLOUR EVOLUTION, ABSOLUTE LUMINOSITY AND BOLOMETRIC LIGHT CURVES

In order to establish the intrinsic luminosity of our sample of supernovae, it is essential to establish their distances, phases and the extent to which they are subject to extinction. We have already estimated the distance moduli (Section 2) and these are listed in Table 1.

As explained in Section 4, prediscovery limits for SNe 1999br and 2001dc allow us to pin down their explosion epochs to within a few days and hence establish clearly the phase of these events at any given date. In addition, below we shall show that the similarity of the

Table 9. Photometry of SN 2001dc (JD +240 0000).

Date	JD	*U*	*B*	*V*	*R*	*I*	Instrument
22/06/01	52083.43	–	21.27 (0.06)	19.84 (0.03)	19.08 (0.01)	18.49 (0.01)	1
04/07/01	52095.42	–	21.22 (0.09)	19.78 (0.03)	19.06 (0.02)	18.42 (0.02)	1
13/07/01	52104.46	–	21.61 (0.08)	19.78 (0.04)	19.00 (0.03)	18.37 (0.02)	1
20/07/01	52111.44	23.65 (0.44)	21.75 (0.04)	19.86 (0.04)	19.02 (0.02)	18.33 (0.02)	2
17/08/01	52139.42	–	22.20 (0.26)	20.00 (0.10)	19.20 (0.07)	18.52 (0.04)	3
18/08/01	52140.39	–	–	20.08 (0.06)	19.20 (0.05)	18.49 (0.03)	4
19/08/01	52141.36	–	22.40 (0.34)	–	–	–	4
27/08/01	52149.32	–	–	20.38 (0.19)	19.44 (0.15)	18.72 (0.05)	4
13/09/01	52166.36	–	$\geqslant$23.95	–	–	–	3
13/09/01	52166.36	–	–	22.16 (0.30)	21.07 (0.13)	20.15 (0.08)	3
08/10/01	52191.26	–	–	–	21.24 (0.27)	21.23 (0.37)	4
09/10/01	52192.33	–	–	–	–	20.20 (0.50)	4
12/10/01	52195.33	–	–	–	21.34 (0.30)	20.55 (0.30)	4
13/10/01	52196.26	–	–	–	–	20.63 (0.15)	4
18/10/01	52201.33	–	–	22.27 (0.65)	21.69 (0.30)	20.70 (0.27)	3
18/10/01	52201.35	–	–	–	–	20.72 (0.27)	3
19/12/01	52262.76	–	–	22.89 (0.30)	22.02 (0.32)	–	3

Notes: 1 = JKT + JAG; 2 = TNG + OIG; 3 = TNG + Dolores; 4 = Asi 1.82-m + AFOSC.

Table 10. Magnitudes of the sequence stars in the field of NGC 5777. The numbers in brackets are the rms of the available measurements. Uncalibrated *U* magnitudes of sequence stars obtained on 2001 July 20 are also reported.

Star	*U*	*B*	*V*	*R*	*I*
1	19.72 (–)	19.68 (0.01)	18.88 (0.01)	18.40 (0.01)	17.94 (0.02)
2	20.45 (–)	20.97 (0.02)	20.56 (0.01)	20.28 (0.01)	20.06 (0.01)
3	–	20.35 (0.01)	19.92 (0.01)	19.64 (0.01)	19.28 (0.01)
4	–	19.24 (0.01)	18.70 (0.01)	18.37 (0.01)	18.04 (0.01)
5	–	20.87 (0.02)	20.42 (0.02)	20.09 (0.01)	19.88 (0.02)
6	21.60 (–)	20.77 (0.01)	19.26 (0.01)	18.33 (0.01)	17.38 (0.01)
7	20.51 (–)	19.71 (0.03)	18.51 (0.01)	17.79 (0.01)	17.10 (0.02)
8	19.22 (–)	19.21 (0.01)	18.33 (0.02)	17.85 (0.01)	17.40 (0.01)
9	19.75 (–)	19.43 (0.01)	18.57 (0.01)	18.02 (0.01)	17.56 (0.02)
10	–	22.16 (0.02)	20.75 (0.02)	19.83 (0.03)	18.87 (0.04)

Table 11. Slope of the light curve of SN 2001dc in the *B*-, *V*-, *R*- and *I*-bands (in mag/100 d). The phase is relative to JD = 245 2047.

Band	35–70	90–120	115–220
γ_B	1.88	–	–
γ_V	0.02	7.97	0.79
γ_R	−0.27	8.00	0.90
γ_I	−0.57	6.17	1.59

spectrum of SN 1999br at a phase of ∼100 d to the earliest available spectra of SNe 1997D and 1999eu allows us to fix the phases of these two events. Likewise, we determined the phase of SN 1994N through the similarity of its earliest spectrum to a spectrum of SN 1999br at ∼30 d. Thus, we deduce that the phases of our five CC-SNe at discovery were: SN 1994N: 31.5 d, SN 1997D: 101.7 d, SN 1999br: 2.9 d, SN 1999eu: 93.5 d, SN 2001dc: 4.5 d.

For extinction, we have argued that for SNe 1994N, 1997D, 1999br and 1999eu we need only consider the effect of the Milky Way ISM. However, to estimate the extinction towards SN 2001dc, we must first consider the colours and colour evolution of the five CC-SNe. This is also valuable as an additional means of testing the degree of homogeneity of the sample. The (*B*–*V*) and (*V*–*R*) colours are shown as a function of phase and compared with those of the peculiar SN 1987A and the 'normal' Type II plateau supernova 1999em in Fig. 10. Corrections for galactic extinction have only been applied to the sample CC-SNe. The SN 1987A and SN 1999em colours have been corrected for the total extinction to these events, using, respectively, $A_V = 0.6$ (West et al. 1987) and $A_V = 0.31$ (Baron et al. 2000). For SN 2001dc, the similarity of its colour *evolution* and its spectra to those of SN 1999br at similar epochs during the plateau phase, plus its location close to a dusty region in NGC 5777, leads us to argue that its redder colours (relative to SN 1999br) are due to strong extinction in the host galaxy (see Fig. 8) as well as in the Milky Way. Therefore, in Fig. 11, we show the same data, but with the SN 2001dc colours dereddened to match those of SN 1999br. From this, we deduce the total reddening to SN 2001dc to be $E(B–V) = 0.42$ and $E(V–R) = 0.33$, corresponding to $A_B = 1.7$. The adopted extinction values for all the SNe are shown in Table 1.

Inspection of Fig. 11 shows that, during the first 100 d, the data are consistent with there being a similar colour evolution for the five sample SNe. During the plateau phase the (*B*–*V*) colour reddens for the first ∼60 d reaching $(B–V) \sim 1.5$. It then remains at about

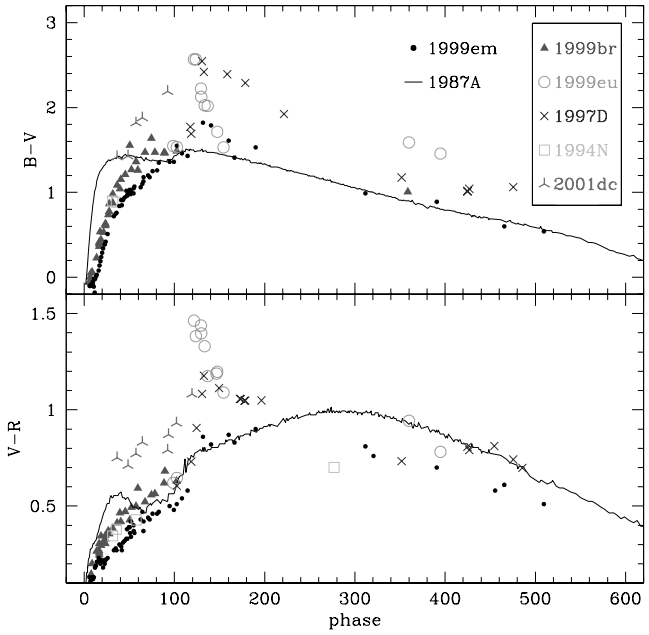

Figure 10. Evolution of (*B*–*V*) and (*V*–*R*) colours of the sample SNe, compared with those of SN 1987A and SN 1999em. The SN 2001dc colours are not plotted beyond ∼120 d because of their large uncertainty. Corrections for galactic extinction only have been applied to the sample CC-SNe. The SN 1987A and SN 1999em colours have been corrected for the total extinction to these events, using, respectively, $A_V = 0.6$ and $A_V = 0.31$.

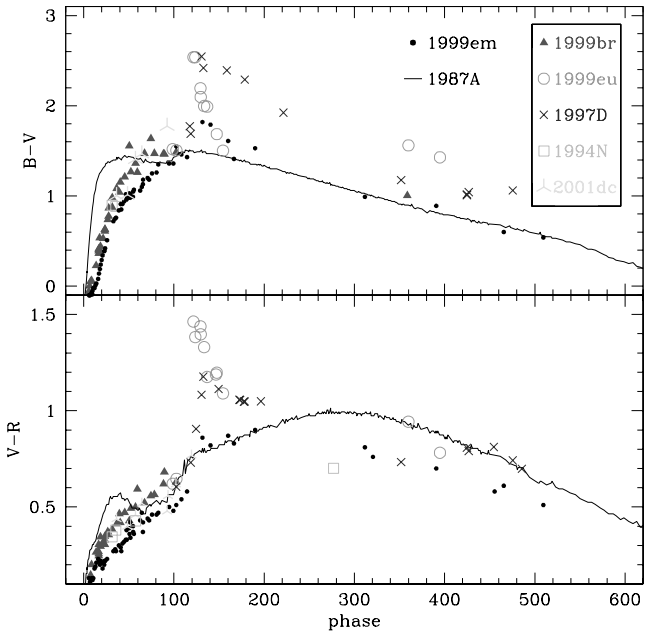

Figure 11. Same as Fig. 10, but correcting for the total extinction towards SN 2001dc, using $E(B–V) = 0.42$, $E(V–R) = 0.33$ magnitudes.

this value for the next 60 d. Beyond ∼100 d, good photometric coverage is available for only two of the five sample SNe, viz. for SNe 1997D and 1999eu. At ∼120 d, the (*B*–*V*) colour of these two events suddenly reddens further to (*B*–*V*) ∼ 2.5. This coincides with the epoch of the steep post-plateau decline (cf. Figs 5 and 12). After this, the (*B*–*V*) colour of these two SNe become bluer, with SN 1999eu showing a particularly rapid change. The plot of (*V*–*R*) versus time shows a rather similar behaviour. SNe 1987A and 1999em show a somewhat different behaviour, and in particular does not show a rapid change at 120–160 d.

Having established the distances, phases and extinctions for the five CC-SNe, we derived M_V light curves for these events. These light curves are plotted in Fig. 12 and compared with those of SNe 1987A and 1999em. It can be immediately seen that for all epochs at which photometry is available, i.e. during both the plateau and nebular phases, the five sample SNe are fainter than both SNe 1987A and 1999em. In the case of SN 1999br, this includes epochs as early as just about one week after explosion. Given that SN 1987A itself was unusually under-luminous, we conclude that our CC-SNe, at least when observed, were all exceptionally faint. For example, during the plateau phase, SN 1999br had a magnitude of just $M_V \approx -13.76$, while for SN 2001dc $M_V \approx -14.29$. We conclude that, in spite of the incomplete coverage of individual light curves, it is likely that the five CC-SNe considered here were all exceptionally subluminous throughout both the plateau phase and the later radioactive tail.

The pseudo-bolometric *'OIR'* light curves (shown in Fig. 13) were computed integrating the emitted fluxes in the *B*-, *V*-, *R*- and *I*-passbands at the epochs for which measurements were available, and interpolating between points adjacent in time when a measurement was missing. In the case of SN 1994N only a single point was available in the *I*-band and the integration had to be restricted to the *BVR*-bands. To illustrate the effect of this limitation, we show also the equivalent *BVR* light curve of SN 1997D as a dotted line. The five SNe are fainter than SN 1987A at any epoch: i.e. the plateau luminosity of SN 1999br (the best monitored event) is $L_{BVRI} \approx 5 \times 10^{40}$ erg s^{-1}, a factor of 10 times lower than the luminosity of SN 1987A at the epoch of the broad maximum. The earlier light curves of SNe 1994N and 2001dc show similar magnitudes and evolution, while SN 1999br is about a factor two times fainter. Between ∼100 and 200 d, SNe 1997D, 1999eu and 2001dc show somewhat different magnitudes and/or evolution. SN 1999eu shows a particularly dramatic drop in luminosity during this time. Between days 270 and 550, the magnitudes and decline rates of SNe 1999br and 1999eu are roughly consistent with their being powered at this time by a small amount of ^{56}Ni (see also Section 7).

6 SPECTROSCOPY

The SNe discussed in this paper have also been observed spectroscopically, and, despite their faintness, later coverage extends into the nebular phase for some events. In this section we present spectra for SNe 1994N, 1999br, 1999eu and 2001dc. We discuss these spectra together with those of SN 1997D (Benetti et al. 2001). In particular, we illustrate the use of spectral similarities to determine the phases of some of the CC-SNe.

6.1 Individual properties

(i) SN 1999br, the supernova for which we have the best coverage at early times, shows the typical features of a Type II event (Fig. 14).

The earliest spectrum indicates a phase of about +10 d post explosion, viz. a blue continuum, with relatively broad P-Cygni lines of H I and Fe II. This is consistent with the phase derived previously from the light curve. The narrow lines arise from poor subtraction of an underlying H II region. During the first month, the spectra exhibit P-Cygni line profiles of H I, Fe II (main lines are identified as: multiplets 27, 28, 37, 38 between λλ4100 and 4700; multiplet 42 at λλ4924, 5018 and 5169; multiplets 48 and 49 at between λλ5200 and 5500; multiplets 40, 74, 162, 163 between λλ6100 and 6500),

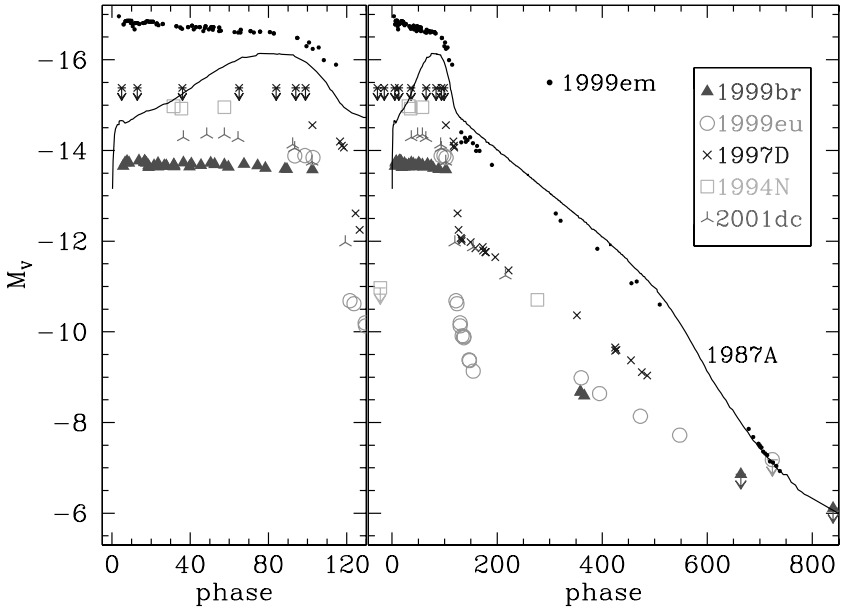

Figure 12. *V*-band absolute light curves of the sample CC-SNe discussed in this paper, SN 1987A and SN 1999em. By comparison of spectra (Section 6), we conclude that the explosion epochs of SNe 1997D, 1999eu and 1994N were, respectively, 101.7, 93.5 and 31.5 d before discovery. Prediscovery upper limits (unfiltered) are also shown along with some late-time upper limits. The SN 1987A light curve (see Patat et al. 1994, and references therein) are corrected for total extinction $A_V = 0.6$, that of SN 1999em (Hamuy et al. 2001; Leonard et al. 2002a; Elmhamdi et al. 2003; Leonard et al. 2003) for $A_V = 0.31$. The SN 2001dc photometry has been corrected for a total estimated extinction of $A_V = 1.28$ (Section 5). The host galaxy extinction for the other 4 SNe is probably negligible, and so the photometry for these SNe has been corrected for Galactic extinction only (Schlegel et al. 1998).

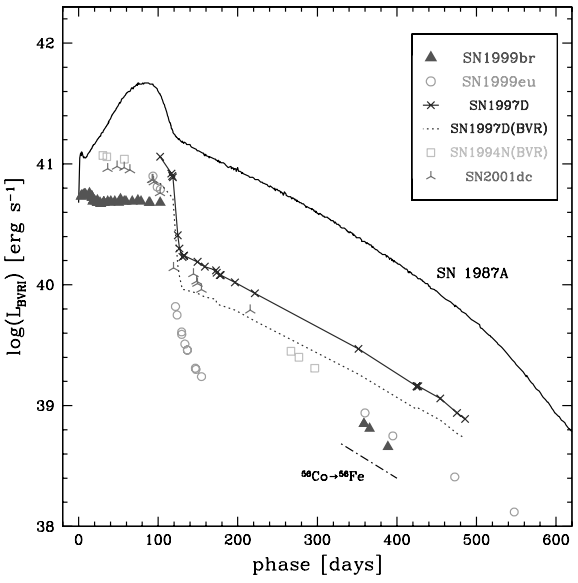

Figure 13. Comparison of the pseudo-bolometric *'OIR'* light curves of the sample CC-SNe. The data of SN 1997D are from Turatto et al. (1998) and Benetti et al. (2001). The bolometric light curve of SN 1987A (Patat et al. 1994, and reference therein) is also shown for comparison. For SN 1994N, the integration is limited to the *BVR* bands. To illustrate the effect of this limitation, we show also the equivalent BVR light curve of SN 1997D (dotted line).

Ca II (H&K and the IR triplet), Na I (λλ5890–5896), Ti II (many multiplets below ∼λ5400), Ba II (multiplet 1 at λλ4554, 4934; multiplet 2 at λλ5854, 6142, 6497) and Sc II (e.g. multiplets 23, 24, 28 with the strong line at λλ6246, 29 with a strong blend at ∼λ5660, 31 with line at λ5527). With age, the continuum becomes redder and the absorption lines become deeper and less blue-shifted. After a gap of 60 d, the final spectrum was taken at about 100 d after explosion, and this shows that a significant evolution had taken place in the intervening interval. Numerous P-Cygni profiles dominate the spectrum, and their narrow width indicates very-low expansion velocities (∼1000 km s^{-1}). The most prominent ones are identified as Ca II, Ba II and Sc II (see Section 6.3). The spectrum at this stage closely resembles that of SN 1997D at discovery (see Fig. 18, later). The line identifications at phase ∼100 d are discussed in detail in Section 6.3.

(ii) Four spectra are available for SN 1999eu (Fig. 15). The first two, taken just after discovery, are strikingly similar to those of SN 1999br at about 100 d post explosion (Fig. 18, later), i.e. the continuum is very red and the lines show expansion velocities of only ∼ 1000 km s^{-1}. The remaining two spectra, taken during the fast post-plateau drop, show even redder continua in agreement with the colour evolution discussed above.

(iii) The earliest two spectra of SN 1994N (Fig. 16) show the typical appearance of Type II SNe during the photospheric phase (Turatto, Gouiffes & Leibundgut 1994). The expansion velocity deduced from the Hα minimum (4500 km s^{-1}) is substantially lower than that measured in 'normal' Type II SNe but is similar to those of SN 1999br 3–4 weeks post explosion. The latest spectrum was taken when the supernova was well into its nebular phase, and is reminiscent of the spectrum of SN 1997D at about 11 months post explosion (Benetti et al. 2001). Besides Hα (FWHM ≈ 1200 km s^{-1}), the main spectral features are the [Ca II] λλ7291–7323 doublet, the Ca II IR triplet, and the strong emission lines of [O I] λλ6300–6364. We also tentatively identify Mg I] λ4571, Hβ, Na I D and [Fe II] λ7155.

(iv) Only three spectra of SN 2001dc are available (Fig. 17), taken during the plateau phase, at ∼54, ∼91 and ∼99 d post explosion. The continuum is red and there is little evolution in the spectral

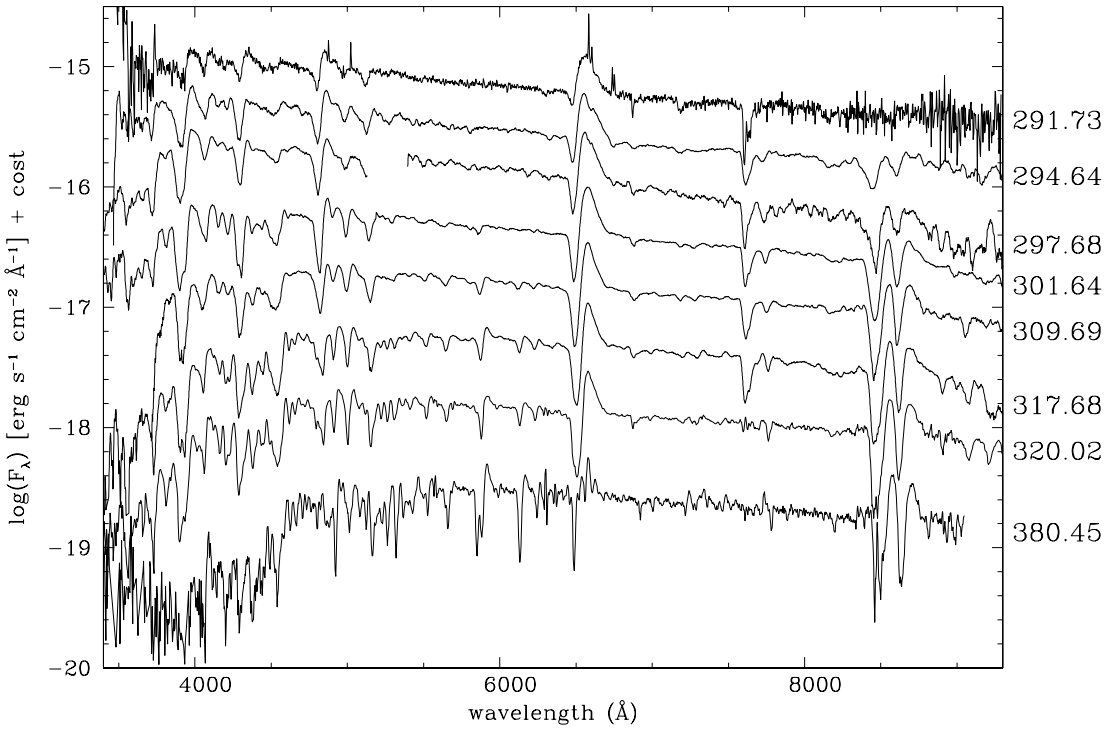

Figure 14. Spectral evolution of SN 1999br. The numbers on the right are JD +245 1000. The sequence of the first 7 spectra covers a period of about one month from discovery, while the last spectrum (1999 July 20, JD = 245 1380.45) is taken 2 months later, at the end of the plateau.

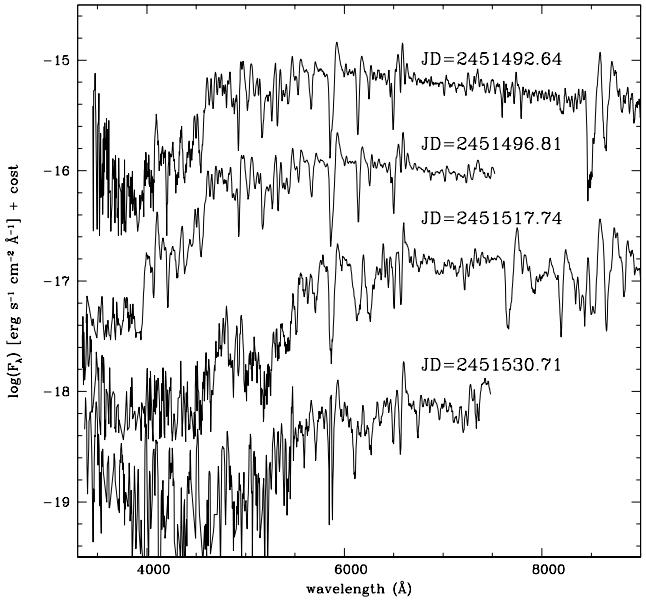

Figure 15. Spectral evolution of SN 1999eu. The spectrum of 1999 December 18 (JD = 245 1530.71) is smoothed because of the poor signal to noise ratio.

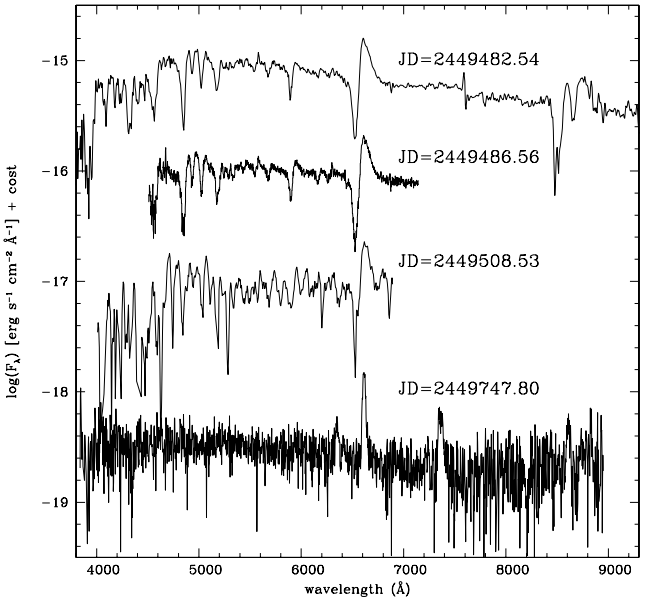

Figure 16. Spectral evolution of SN 1994N. The spectrum of 1994 June 5 (JD = 244 9508.53) is smoothed because of the poor signal to noise ratio.

features during this time interval. The last two spectra of SN 2001dc resemble those of 1999br and SN 1999eu at ∼100 d post explosion, especially the strong and narrow P-Cygni lines of Ba II and Sc II. These spectra correspond to the beginning of the departure from the plateau phase. A strong P-Cygni line is present in the last spectrum with its emission peak at ∼λ9245. We tentatively identify this with Sc II λ9234.

In Fig. 18, we compare the spectra of SN 1997D (1997 January 15), SN 1999br (1999 July 20) and SN 1999eu (1999 November 14). It can be seen that these are strikingly similar both with respect to the continua and the line components. We suggest, therefore, that these spectra were acquired at similar phases (see also Zampieri et al. 2003). The light curves of these SNe indicate that this phase was probably about the end of the plateau phase, with the

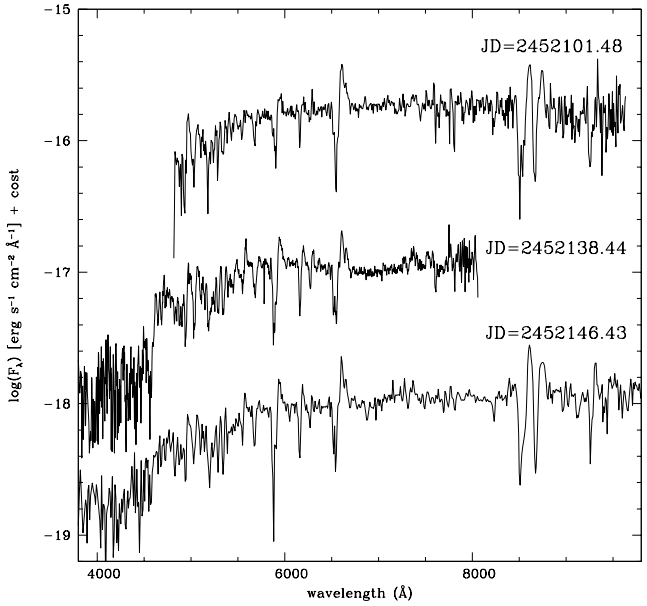

Figure 17. Spectral evolution of SN 2001dc. The spectra have not been corrected for reddening.

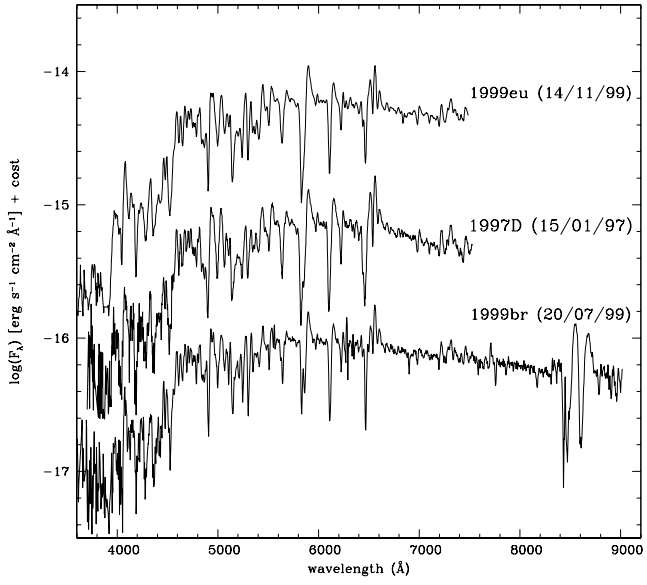

Figure 18. Spectra of SN 1999eu, SN 1997D and SN 1999br at about the end of the plateau.

SN 1999br light curve indicating that this was ∼100 d post explosion. For SN 1994N, in spite of the paucity of observations, comparison of the first spectrum taken on 1994 May 10 with a spectrum of SN 1999br obtained on 1999 May 11 suggests that SN 1994N was discovered about one month after the explosion. Indeed the two spectra show the same features and similar expansion velocities (∼2500 km s^{-1}, deduced from the minimum of the Fe II λ5018 line). The adopted epochs of explosion for all five CC-SNe are given in Table 1. These were used in the analysis of colour and light curves in Section 5.

6.2 The common spectrophotometric evolution of the low-luminosity Type II SNe

We have used similarities in the spectra of the low-luminosity SNe to date the explosions. In order better to illustrate the properties of this group of SNe, we now use all the available data to describe the general spectrophotometric evolution of this class. In Fig. 19 we show the temporal evolution of selected spectral windows.

The first ∼40 d of evolution (spectra 1–8) are covered mainly by the SN 1999br spectra (cf. also Fig. 14). The spectra evolve from a continuum dominated by Balmer lines to a more complex appearance with strong lines of Na I, Ba II and the Ca II IR triplet. The expansion velocities are relatively low compared with 'normal' Type II SNe, slowing from 5000 to 3000 km s^{-1} during this early era. The spectra of SN 1994N (No. 5) and SN 2001dc (No. 8) fit well into the evolutionary sequence of SN 1999br. During this phase, the absorption trough velocities exhibit rapid movement towards lower velocities (see Fig. 19 and below).

The next spectrum (No. 9) takes us well into the second half of the plateau phase. Clearly, the spectroscopic form has changed significantly in the intervening ∼37 d. The remainder of the plateau era (spectra 9–12 in Fig. 19) is represented by a single spectrum each from SNe 1997D, 1999br, 1999eu and 2001dc. As described earlier, we used the relative similarity of these spectra at about this epoch to pin down the phases of SNe 1997D and 1999eu. By this time (phase ∼80–100 d), the absorption troughs of the more prominent lines indicate relatively low velocities at the photosphere, e.g. Hα and Sc II λ6246 give velocities of ∼1000–1500 km s^{-1} (Fig. 20). In addition, new narrow lines of low-excitation elements like Ba II, Sc II, Fe II, Sr II and Ti II have appeared (see also Figs 23–26, later) and the continuum becomes redder (see e.g. Fig. 14). In particular the Ba II lines become the strongest features in the spectra. Note that the contribution of Sr II at short wavelengths is also supported by the detection of strong lines of multiplet 2 (at λλ10037, 10327 and 10915) in the IR spectrum of SN 1997D presented by Clocchiatti et al. (2001).

The evolution up to about one month after the plateau (spectra from about 13 to 16) is characterized by the transition to a nebular spectral form, with the gradual fading of permitted metallic lines and P-Cygni profiles. In this phase, narrow forbidden lines have steadily strengthened (in particular [O I] λλ6300–6364 and [Ca II] λλ7291–7323, but also some multiplets of [Fe I], [Fe II] and Mg I]), as reported also in fig. 5 of Benetti et al. (2001).

The spectra of the latest phase (Nos 17–20) resemble those of normal Type II SNe, with the usual (though narrower) emission features attributed to forbidden transitions (Turatto et al. 1993). Nevertheless, the most prominent line is Hα, and Na I D is still visible as a faint emission line after almost 1.5 yr.

A comparison between the spectra of the faint Type II SNe with those of SN 1987A at comparable phases is shown in Fig. 21. At the ∼20- and ∼90-d epochs, the main spectral lines are the same, but the lines of our subluminous CC-SNe have narrower widths – implying lower ejecta expansion velocities. In addition, at ∼90 d the subluminous SNe show stronger absorption components of Ba II. As noted by Turatto et al. (1998) for SN 1997D, this is probably not an effect of overabundance, but is simply a consequence of a lower ejecta temperature.

We conclude that a characteristic property of subluminous CC-SNe is the very-low expansion velocity of the ejecta. Indeed the photospheric velocities inferred from the absorption minima of Hα and Sc II λ6246 show a common evolutionary path (Fig. 20). During the first ∼50 d the line velocities decrease monotonically from 5000

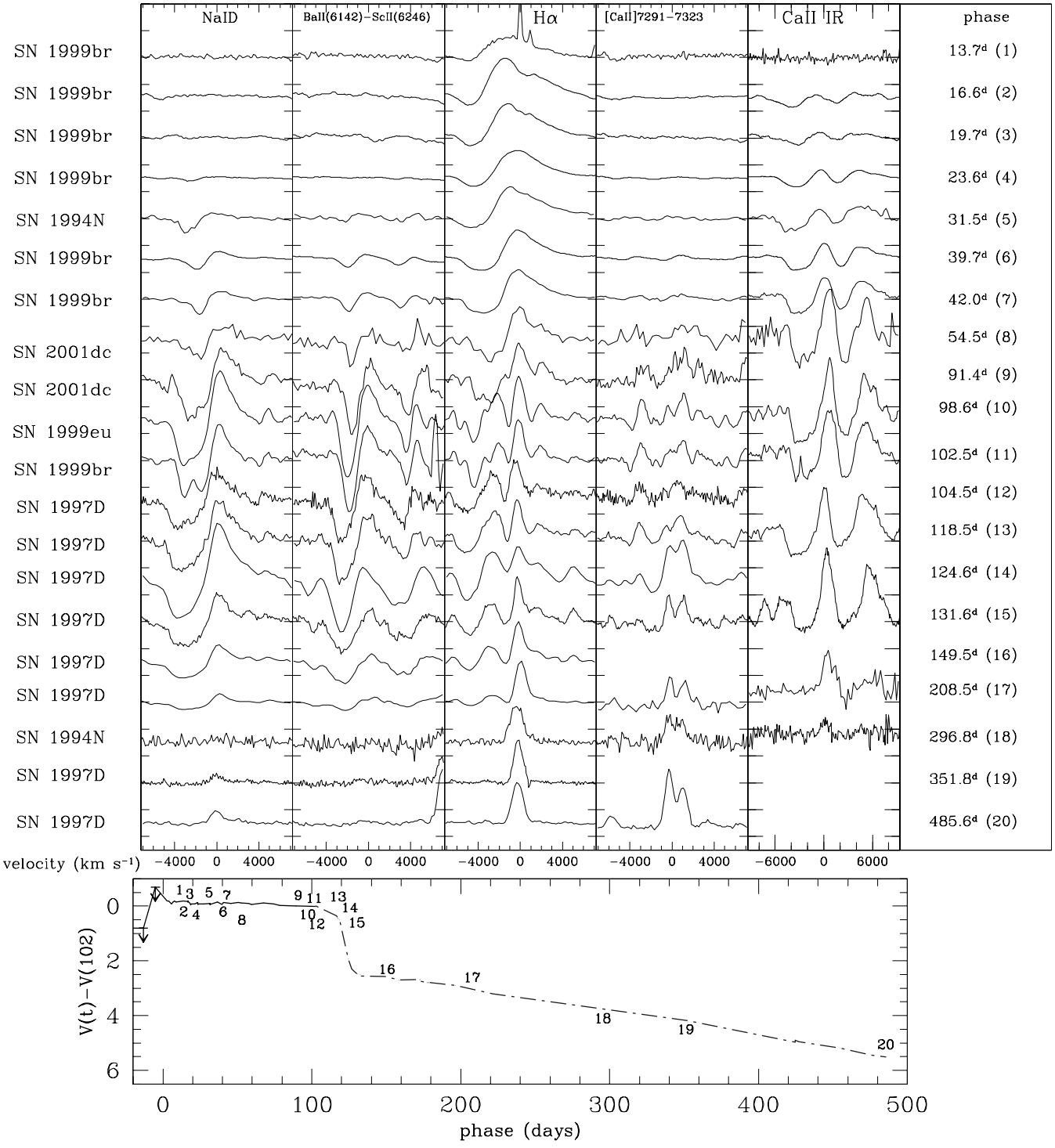

Figure 19. Top: evolution of selected regions of the spectra of low-luminosity Type II SNe. The name of the supernova is given in the left column, while the phase (relative to the explosion epoch) is on the right. The numbers in brackets correspond to the epochs shown on the schematic light curve (bottom panel), obtained by combining the *V*-band light curve of SN 1999br (solid curve) and SN 1997D (line–dot curve). The magnitudes of both SNe are scaled so that their *V*-magnitudes match at phase ∼102 d post explosion.

to 1000–1500 km s^{-1}. Somewhere towards the end of the plateau the velocities level off at a value $\leqslant$1000 km s^{-1}. At all epochs, line velocities are lower than those of the 'typical' II-P SN 1999em (cf. Fig. 20).

We have also analysed the continuum temperature from the spectra of the SNe by performing a Planckian fit in regions not affected by line blanketing (e.g. between about λλ6000 and 8000). The results, shown in Fig. 22, are fairly consistent with a common evolution. Starting from a value of ∼8000 K at phase ∼13 d, the temperature falls, reaching 5000–6000 K after 30–40 d. During the remainder of the plateau the temperature remains almost constant at ∼5500 K. Presumably this corresponds to the recombination temperature of

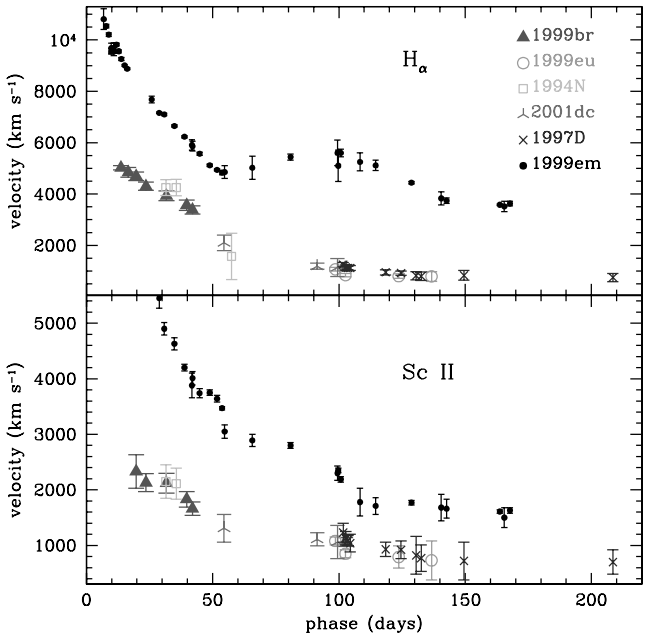

Figure 20. Photospheric velocity of low-luminosity Type II SNe deduced from the minima of P-Cygni absorption of Hα and Sc II 6246 A and comparison with SN 1999em (data from the Padova-Asiago SNe Archive and Leonard et al. 2002a). The x-axis shows the phase with respect to explosion.

the hydrogen as the photosphere recedes through the H envelope. The end of the plateau phase is marked by the onset of a steep temperature decline, settling at $T\sim$ 4000 K as the supernova enters its nebular phase.

6.3 Identification of the spectral lines

The multiplicity of narrow P-Cygni features in the late photospheric spectra of the faint Type II SNe can help us to identify unambiguously the species responsible. To exploit this opportunity we have modelled the spectra of SN 1999br at phase 102.5 d.

We used the parametrized code SYNOW (Fisher 2000) to construct synthetic photospheric spectra, which were then compared with the observations. The code works in the Sobolev approximation and includes a number of simplifying assumptions. The line-forming envelope surrounding the continuum-emitting region expands homologously and with spherical symmetry. The line source function is taken to be that of resonance scattering. The optical depth τ of the strongest optical line of each ion is a free parameter. For all the other lines of a given ion, τ is found assuming Boltzmann excitation (Jeffery & Branch 1990). Other free parameters are the velocity at the photosphere ($v_{\rm ph}$), the continuum blackbody temperature ($T_{\rm bb}$), the excitation temperature ($T_{\rm exc}$) of each ion and the radial dependency of the optical depths. We adjusted these parameters to produce a plausible spectral match to the ∼102-d spectrum of SN 1999br. In the final model we adopted a power-law radial dependency of

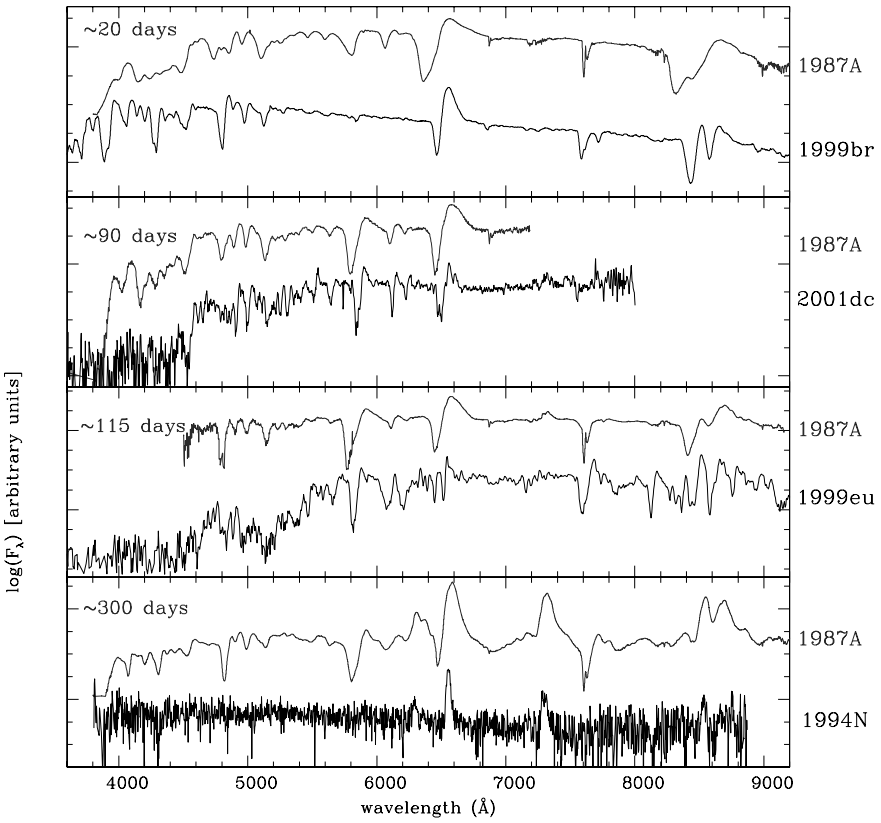

Figure 21. Comparison of the spectra of SN 1987A with those of faint Type II SNe at similar phases. The phases with respect to the explosion epoch are shown in the upper-left corner.

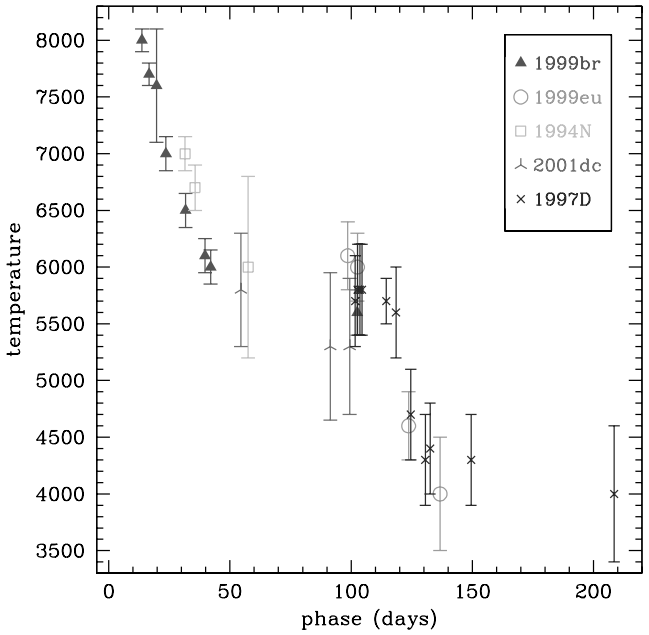

Figure 22. Evolution of continuum temperature derived from Planckian fits to the SNe spectra. The continuum of SN 2001dc is corrected for reddening of $A_{\rm B,tot} = 1.7$, as discussed in Section 5. The x-axis shows the phase with respect to explosion.

index $n = 4$ with $T_{\rm bb} = 5600$ K and $v_{\rm ph} = 970$ km s^{-1}; $T_{\rm exc}$ varies among the ions, but it is about 4000–5000 K for neutral ions and 8000–10000 K for ionized species.

The resulting spectral model, obtained including 22 different ions, is compared with the whole observed spectrum in Fig. 23, and with expanded sections shown in Figs 24–26. The main spectral features are generally quite well reproduced. In addition the strong line-blanketing behaviour in the blue ($\lambda \leqslant 4600$ Å) is, at least qualitatively, also seen in the model (Fig. 24).

The line-blanketing is due to the presence of many strong metallic lines, including contributions from neutral and singly-ionized ions of Fe, Ti, Cr, Sc, Mn, Ca and Sr. The Sr II lines are particularly deep, while the Balmer lines are fainter than is observed in normal Type II SNe. The region between $\lambda\lambda$4600 and 6500 (Fig. 25) is dominated by lines of Fe II, Ti II, Sc II and Ba II, although contributions from lines of neutral ions cannot be excluded. At this phase the absorption lines of Ba II are exceptionally strong, exceeding in depth the Na I D and Hα lines. The reproduction of the spectrum in the Hα region is poor due to the inadequacy of the pure resonance-scattering assumption for the Hα line. Nevertheless, to reproduce the complex profile in this region, we require the simultaneous presence of Ba II, Hα and Sc II.

On the red tail of Hα up to $\sim\lambda$7700 (Figs 25 and 26) many narrow, faint Ti II and Fe II lines are superimposed on a strong continuum. However, also present may be growing contributions from nebular emission lines, in particular [Fe II] and [Ca II] $\lambda\lambda$ 7291, 7324. As we move still further to the red, the spectrum becomes dominated by the Ca II IR features. Other tentatively identified lines include: K I, O I, Mg II, Na I, C I, Fe I, Fe II, Ba II and Ti II (Fig. 26).

7 DISCUSSION

Following our determination of the explosion epochs, we can conclude that our observations are consistent with low-luminosity SNe having plateaux of duration $\sim$100 d, similar to that seen in more normal II-P SN events. This may constitute evidence for the presence of massive envelopes around low-luminosity SNe (Zampieri et al. 2003). We attribute a $\sim$100-d plateau to SN 1997D. This is significantly longer than that estimated by Turatto et al. (1998) and Benetti et al. (2001). In general, the plateau luminosities of the faint CC-SNe are unusually low, and show a range of values between the different events spanning more than 1 mag (see Section 5, Figs 12 and 13). Although spectroscopic coverage is incomplete for individual events, the data are consistent with the low-luminosity SNe having a similar spectroscopic evolution, characterized by unusually narrow linewidths.

At the end of the plateau the light curves show a steep decline, typically 3 mag in 30–50 d. This effect has also been observed in other II-P SNe (e.g. SN 1994W, Sollerman et al. 1998; SN 1999em, Elmhamdi et al. 2003). Thereafter, for three of the four SNe for which we have post-plateau light curves, the decline rate is consistent with the power source being the radioactive decay of ^{56}Co. The exception is SN 1999eu, discussed below. Assuming complete trapping of the γ-rays, we compare the *'OIR'* pseudo-bolometric luminosities (Fig. 13) with those of SN 1987A at similar epochs and, using the relation

$$M_{\rm SN}({\rm Ni}) = 0.075 \times \frac{L_{\rm SN}}{L_{\rm 87A}}\,{\rm M}_{\odot},$$

we obtain the following useful lower limits for the ejected ^{56}Ni masses: $\sim$0.008 M$_\odot$ for SN 1997D, $\sim$0.002 M$_\odot$ for SN 1999br, $\sim$0.006 M$_\odot$ for SN 1994N (using only the *BVR* bands) and $\sim$0.006 M$_\odot$ for SN 2001dc (with a large uncertainty due to poor late time photometry). We note that the value for SN 1997D is a factor of four higher than the value estimated by Turatto et al. (1998) owing to differences in estimated explosion epoch and distance (see Table 1 for new estimates). By analogy with SN 1987A, we can deduce that no more than 50 per cent of the luminosity was lost in unobserved bands. Consequently, we may conclude that a common feature of these events is ejection of a very-low ^{56}Ni mass.

As mentioned above, SN 1999eu is noticeably different from either SN 1997D or SN 2001dc in that it exhibits a particularly large post-plateau decline of about 5 mag. The large decline refers to the entire duration of the observations prior to the disappearance of SN 1999eu behind the sun. It's remarkable that a similar behaviour has already been observed in SN 1994W (Sollerman et al. 1998). Moreover, its luminosity drops to a level about three times lower than would be expected from a simple backward extrapolation of the later ^{56}Co radioactively-driven tail. Two possible explanations present themselves. One is the early condensation of dust in the ejecta, causing much of the luminosity to be shifted into the unobserved mid- and far-infrared. Then, as the ejecta expanded, the dust became optically transparent to the optical luminosity and so the light curve increasingly followed the radioactive decline rate, with a luminosity corresponding to 0.003 M$_\odot$ of ^{56}Ni. A similar phenomenon was seen in SN 1987A but at a later epoch. Difficulties with the dust hypothesis are: (a) the rather early epoch of the condensation, while the temperature is still rather high in at least some of the ejecta; (b) its rather 'convenient' coincidence with the decline at the end of the plateau. Unfortunately, nebular spectra of SN 1999eu are not available and so we cannot check for the occurrence of a red-wing truncation, which dust condensation might be expected to produce (cf. SN 1987A and SN 1999em). The second possibility is that the late-time tail is, in fact, powered mostly by ejecta–CSM interaction and not by radioactive decay. This would imply an extremely low ejected mass of ^{56}Ni (<0.001 M$_\odot$). A possible difficulty is that if

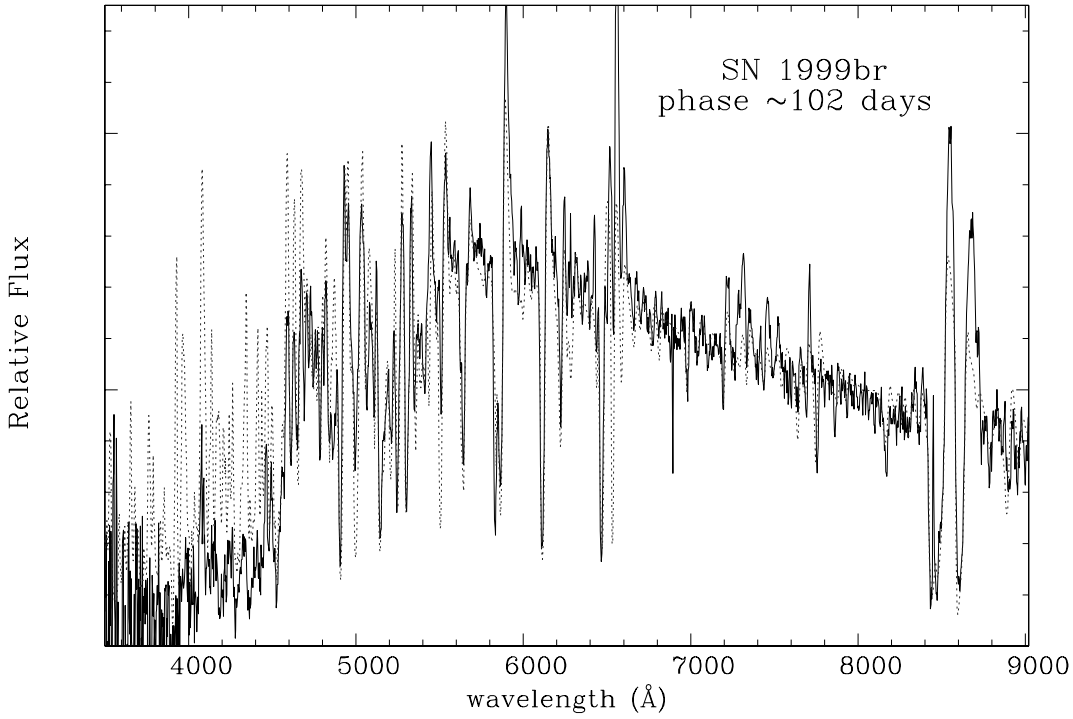

Figure 23. Comparison between the observed spectrum of SN 1999br at phase ∼102 d and the SYNOW synthetic spectrum. The solid curve is the observed spectrum, corrected for redshift, the dotted curve is the synthetic one.

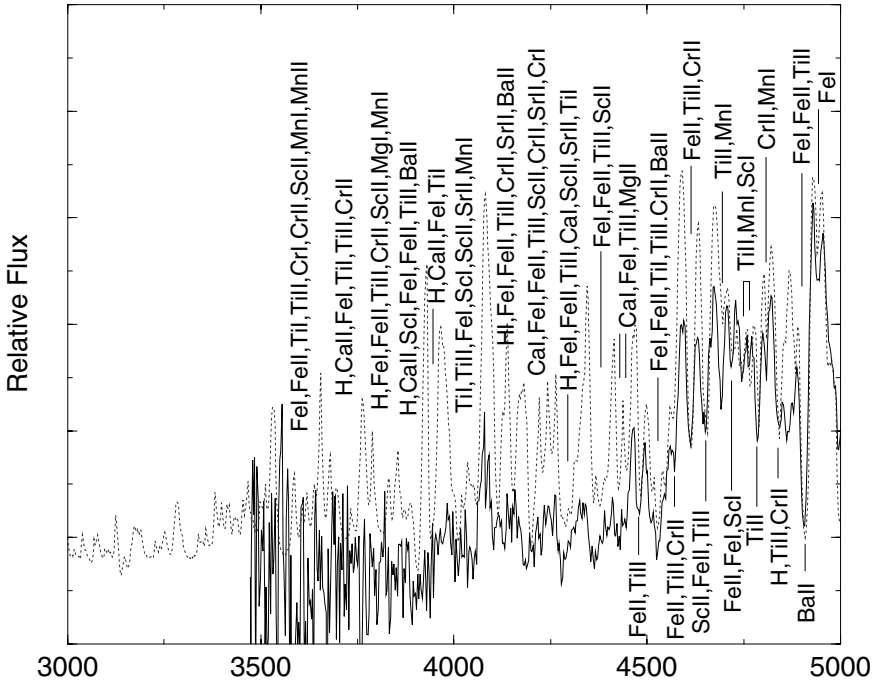

Figure 24. Line identification in the wavelength region λλ3000–5000 for the spectra shown in Fig. 23.

the light curve is being mostly driven by such an interaction, then there is no obvious reason for its being close to the decay rate of ^{56}Co between 350 and 550 d.

In summary, the group of five CC-SNe considered here are similar to more typical CC-SNe in that a clear plateau phase occurs lasting for ∼100 d, followed by a late-time decline driven by the decay of ^{56}Co. A similar temperature behaviour is seen (Fig. 22), and the identities of the spectral lines at all phases are also typical. However, these SNe differ in that (a) during the plateau phase the luminosity is at least a factor 10 times less than found in typical CC-SNe, (b) the expansion velocity is unusually slow (Fig. 20), both during the photospheric and nebular phases, and (c) the mass

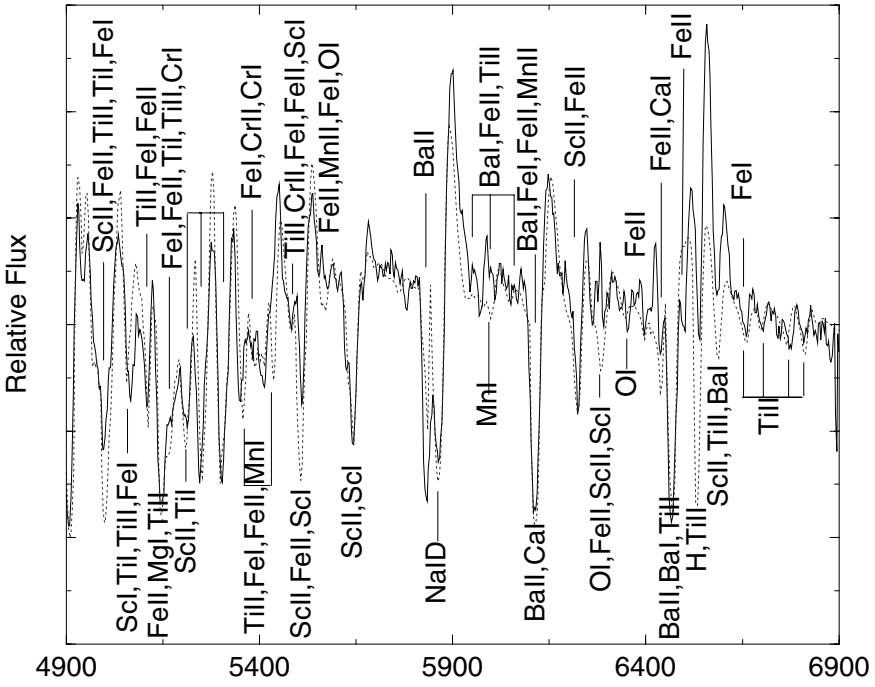

Figure 25. Like Fig. 24, but in the wavelength range λλ4900–6900.

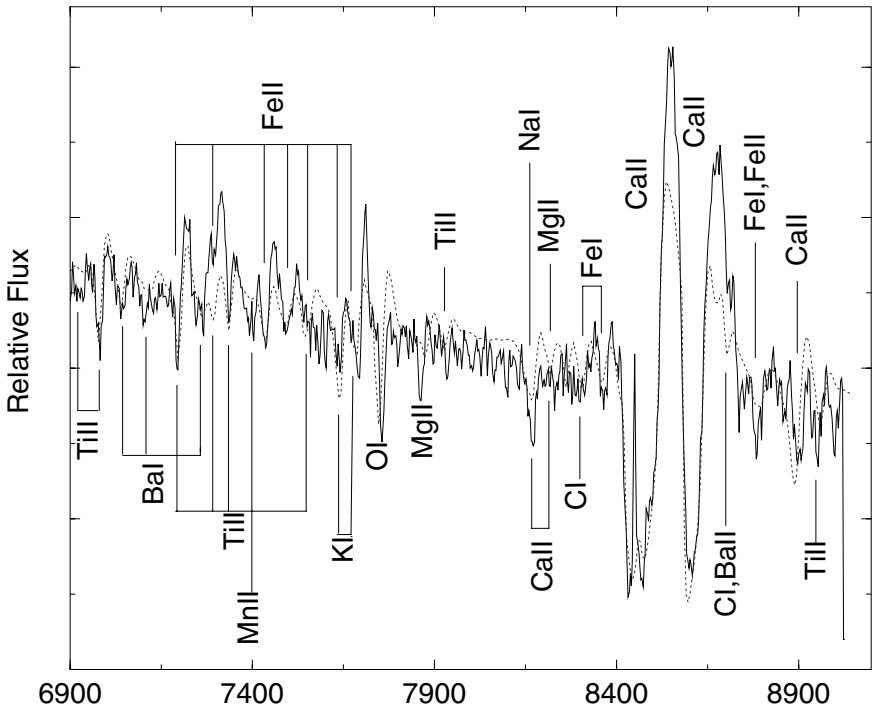

Figure 26. Like Fig. 24, but in the wavelength range λλ6900–9000.

of ^{56}Co that drives the late-time tail is at least a factor ∼10 lower than normal.

A key issue to address is whether or not the five low-luminosity CC-SNe are members of a separate class of CC-SNe arising from a distinctly different progenitor type and/or explosion process, or whether they are simply samples from the extreme low-luminosity tail of a continuous distribution of otherwise normal explosions. We are currently investigating this problem through the study of Type II SNe having luminosities intermediate between normal objects (like SN 1988A or SN 1969L) and the faint events discussed here. Hamuy (2003) has already considered 24 Type II plateau SNe, deriving a wide range of plateau luminosities (∼5 mag), expansion velocities (∼×5) and ejected ^{56}Ni masses (>×150). His sample includes two of our low-luminosity events, viz. SNe 1999br and 1997D. He found

that both the mid-plateau M_V and ejecta velocity correlate with the mass of ^{56}Ni ejected as deduced from the exponential tail. For a subset of 16 II-P SNe the explosion energy and total ejected mass also correlate with the observed properties of plateau luminosity and velocity. Hamuy asserts that the physical properties of II-P SNe exhibit a continuous range of values, and concludes that II-P SNe form a one-parameter family. We note that the four low-luminosity SNe for which we have a fair estimate of M_V follow the trend of M_V at 50 d versus $M(\mathrm{Ni}^{56})$ shown in Hamuy's fig. 3. It therefore seems reasonable to incline towards the single continuous distribution scenario. Given Hamuy's correlation between ejecta kinetic energy and mass of ^{56}Ni ejected, this implies that low-luminosity CC-SNe are also low-energy events. Similar results for a large sample of II-P SNe support Hamuy's conclusion that a continuous trend of physical parameters in II-P SNe exists, also including extremely-low and moderately-low-luminosity events (Zampieri et al., in preparation).

To account for the low-luminosity CC-SNe, a natural approach is to examine the extreme ends of the mass spectrum of progenitors from which II-P SNe are believed to arise. The high-mass scenario has been proposed by Turatto et al. (1998), Benetti et al. (2001) and Zampieri et al. (2003). Turatto et al. (1998) found that the observed behaviour of SN 1997D could be reproduced by the explosion of a progenitor with $M > 25$ M$_\odot$, radius $R \leqslant 300$R$_\odot$ and explosion energy $E \approx 4 \times 10^{50}$ erg. They also suggested that the central remnant was a black hole (BH) and that significant fallback of stellar material on to the collapsed remnant may have taken place. Zampieri et al. (2003) studied the behaviour of both SN 1997D and SN 1999br. They found that the light curves and the evolution of the continuum temperature and expansion velocity are well reproduced by a comprehensive semi-analytical model in which the envelope is $\leqslant 10^{13}$ cm (140 R$_\odot$), the ejecta masses are $\sim$14–20 M$_\odot$ and the explosion energy is $E \leqslant 10^{51}$ erg. They deduced somewhat lower progenitor masses than did Turatto et al., estimating a progenitor with mass $\geqslant$19 M$_\odot$ for SN 1997D and $\geqslant$16 M$_\odot$ for SN 1999br. From the large ejected masses and low explosion energy, Zampieri et al. conclude that SN 1997D and SN 1999br are intermediate-mass, BH-forming CC-SNe.

A contrary conclusion was reached by Chugai & Utrobin (2000). In their analysis of the early- and late-time spectra of SN 1997D, they found that model spectra for a supernova resulting from a 24- M$_\odot$ progenitor were incompatible with the observed nebular spectra. They also considered a low-mass progenitor model in which the observed behaviour of SN 1997D is reproduced by the low-energy explosion ($E \approx 10^{50}$ erg) of a low-metallicity progenitor. The star has a radius $R \leqslant 85$ R$_\odot$ and a total main sequence mass of $M =$ 8–12 M$_\odot$ (of which 6 M$_\odot$ becomes H-rich ejecta). In this case, the remnant is expected to be a neutron star. They found that this model gave more successful reproduction of the spectra at both early and late times. However, in their analysis Chugai & Utrobin assumed a plateau duration of $\sim$60 d. The new observational evidence provided here and in Zampieri et al. (2003) indicates that the plateau of low-luminosity SNe is $\gtrsim$100 d. Therefore, it is not clear if the low-mass model may still be able to reproduce the observations with such a long plateau duration.

Incidentally, Cappellaro, Barbon & Turatto (2003) find that roughly 50 per cent of low-luminosity II-P SNe occur in late type (Sc) galaxies where recent star formation has occurred, whereas the fraction for normal Type II SNe is only $\sim$15 per cent. This favours a high-mass progenitor for the low-luminosity events.

Ultimately, it may be possible to devise new observational tests for the high-mass scenarios. Woosley & Weaver (1995) have shown, for a low-energy explosion occurring in a massive progenitor, a considerable fraction of ^{56}Ni and other heavy elements may indeed remain gravitationally bound to the compact core and fall back on to it. If the fallback is too large it can lead to problems in reproducing the observed barium and other *r*-process elements (Qian & Wasserburg 2002). However, hydrodynamic calculations show that 1 M$_\odot$ of stellar material can easily remain bound and accrete on to the core, forming a BH. In principle one might detect such a BH via the late-time light curve when accretion luminosity induced by the fallback overcomes the radioactive decay luminosity (Zampieri, Shapiro & Colpi 1998a). For spherical symmetry, the accretion luminosity is predicted to decay as $t^{-25/18}$ (Zampieri et al. 1998b), but it is also not expected to dominate the radioactive luminosity until $\sim$3 yr post explosion (Balberg, Zampieri & Shapiro 2000). Consequently, this effect is currently at the sensitivity limit of the largest ground-based telescopes.

8 ARE LOW-LUMINOSITY SNE RARE?

A significant fraction of all types of SNe may be underluminous, but their faintness may produce a statistical bias against the discovery of such events (Schaefer 1996). Richardson et al. (2002) found that for SNe in our Galaxy and in nearby galaxies ($\mu \leqslant 30$), possibly more than 20 per cent have an intrinsic M_B fainter than –15. The majority of these events are of Type II-P (both 1997D-like and 1987A-like events). Chugai & Utrobin (2000) speculate that the Galactic supernovae of 1054 and 1181 might have been sub-luminous events similar to SN 1997D. They estimate that such faint SNe make up $\sim$20 per cent of all II-P SNe.

The analysis of archival data and published material suggests that several other 1997D-like events have been observed in the past. For example, SN 1973R (Ciatti & Rosino 1977) exhibited low plateau luminosity, relatively narrow P-Cygni lines and a light and colour curve behaviour similar to that of SN 1997D, suggesting that it belongs to this group of sub-luminous SNe. Other candidates might be SN 1923A (Patat et al. 1994), SN 1978A (Elliott et al. 1978), SN 1999gn (VSNET data; Ayani & Yamaoka 1999; Dimai & Li 1999), SN 2000em (Strolger et al. 2000), SN 2001R (Matheson et al. 2001; Weisz, Modjaz & Li 2001) and the recent SN 2003Z (Matheson et al. 2003; Boles et al. 2003). We note, in particular, that the spectroscopic evolution of SN 2003Z closely resembles that of SN 1999br (Pastorello et al. 2003) and that the spectrum of SN 2000em[1] taken by the NGSS team shows many features that are reminiscent of those observed in SN 1997D. The Hα emission dominates with respect to the Ba II λ6497 line, thus resembling e.g. spectra (8) and (9) in Fig. 19.

SN 1978A (Elliott et al. 1978) exhibited narrow P-Cygni spectral features resembling those of SN 1997D. A complex sequence of narrow absorption and emission lines are visible in a rather noisy spectrum (resolution $\sim$10 A). SN 1978A is also peculiar in that while its late-time luminosity was similar to that of 1997D-like events, at discovery its absolute magnitude was much higher: ~ -18.6 (Gilmore 1978; Zealey & Tritton 1978). A possible explanation could be an early interaction with a thin circumstellar shell ejected just before the SN explosion, powering the luminosity at very early phases. However, in this scenario it is difficult to explain the observed low expansion velocities at just 2–3 weeks post explosion. SN 1994W (Sollerman et al. 1998) is also a case where the luminosity at maximum was high, but where a low ($M_{\mathrm{Ni}} \leqslant 0.015$ M$_\odot$) or very-low

[1] http://www.ctio.noao.edu/~ngss/ngss4/ngss4.html

($M_{\rm Ni} \leqslant 0.0026$ M$_\odot$) mass of radioactive ^{56}Ni was ejected, depending on the contribution to the luminosity of an ejecta–CSM interaction.

The discovery in the past few years of a few SNe spectroscopically classified as 1997D-like events suggests that the rate of such events is significant. Among Type II SNe discovered during 1992–2001 in a volume-limited sample (recession velocities $\leqslant$4000 km s^{-1}) (Barbon et al. 1999, and recent updates), at least five are spectroscopically similar to SN 1997D. This suggests that the incidence of such very-low-luminosity events is about 4–5 per cent of all Type II SNe.

9 CONCLUSIONS

In this paper we have presented photometric and spectroscopic observations of four new Type II SNe, viz. SNe 1999br, 1999eu, 1994N and 2001dc. Together with SN 1997D, we have shown that they form a group of exceptionally-low-luminosity events. The discovery of these faint SNe is difficult and their monitoring requires in general large telescopes and long integration times. Partly in consequence of this, the temporal coverage of individual supernovae has been erratic and incomplete. However, taken together, they suggest a fairly homogeneous set of properties, and provide a reasonably complete picture of the photometric and spectroscopic evolution of this type of supernova. Establishment of the phase of these events was important, and the best-observed SN 1999br was particularly valuable in this regard (see also Zampieri et al. 2003).

We find that the group of five CC-SNe considered here are similar to more typical CC-SNe in that a clear plateau phase occurs lasting for $\sim$100 d, followed by a late-time decline driven by the decay of ^{56}Co. A similar temperature behaviour is also seen. The spectrum evolves from a relatively normal Type II SN photospheric spectrum to one characterized by narrow lines ($v \approx 1000$ km s^{-1}), a red continuum and strong Ba II lines. These SNe are unusual in that during the plateau phase the luminosity (both V-band and bolometric) is less by at least a factor of 10 than found in typical CC-SNe. In addition, the expansion velocity is unusually slow both during the photospheric and nebular phases. At the earliest epochs, the photosphere is located at layers expanding at $\sim$5000 km s^{-1}, but within two months it recedes to $v \sim 1000$ km s^{-1}. The mass of ^{56}Co that drives the late-time tail is lower by at least a factor of $\sim$10 than normal, indicating ejected masses of ^{56}Ni in the range 2–8 $\times$ 10^{-3} M$_\odot$.

Comparison with a sequence of more normal Type II SNe (Hamuy 2003; Zampieri et al., in preparation) suggests that this group of SNe represent the extreme low-luminosity tail of a single continuous distribution. This indicates that the low-luminosity CC-SNe are also low-energy events. Although evidence for a low-mass progenitor of low-luminosity CC-SNe may not be completely ruled out yet, recent work seems to support a high-mass progenitor scenario (Zampieri et al. 2003).

Finally, we note that selection effects probably limit the rate of discovery of low-luminosity SNe, and that their true incidence may be as high as 4–5 per cent of all Type II SNe.

ACKNOWLEDGMENTS

This paper is based on observations collected at ESO – La Silla (Chile), ESO VLT – Cerro Paranal (Chile), CTIO (Chile), TNG, WHT and JKT (La Palma, Canary Islands, Spain) and Asiago (Italy). We acknowledge support from the MIUR grant Cofin 2001021149, and partial support from NSG grants AST-9986965 and AST-0204771, and NASA grant NAG5-12127.

We are grateful to M. Hamuy & M. M. Phillips for providing their data for SN 1999br before publication and to the referee D. C. Leonard for helpful comments that have improved the paper. We thank D. Bramich, L. Contri, R. Corradi, S. Desidera, P. Erwin, B. Garcia, E. Giro, D. Lennon, L. Lessio, N. O'Mahoney, J. Rey and A. Zurita for technical support and assistance in the observations of SN 2001dc. AP thanks the University of Oklahoma for generous hospitality.

We are grateful to the VSNET observers, in particular for the useful information about SN 1999eu.

This research has made use of the LEDA data base and of the NASA/IPAC Extragalactic Database (NED), which is operated by the Jet Propulsion Laboratory, California Institute of Technology, under contract with the National Aeronautics and Space Administration.

REFERENCES

Arnett W. D., 1980, ApJ, 237, 541
Arnett W. D., 1987, ApJ, 319, 136
Arp H., 1966, ApJS, 14, 1
Ayani K., Yamaoka H., 1999, IAU Circ, 7336
Balberg S., Zampieri L., Shapiro S. L., 2000, ApJ, 541, 860
Baldwin J. A., Stone R. P. S., 1984, MNRAS, 206, 241
Barbon R., Benetti S., Cappellaro E., Patat F., Turatto M., Iijima T., 1995, A&AS, 110, 513
Barbon R., Buondí V., Cappellaro E., Turatto M., 1999, A&AS, 139, 531
Baron E. et al., 2000, ApJ, 545, 444
Benetti S., Cappellaro E., Turatto M., 1991, A&A, 247, 410
Benetti S. et al., 2001, MNRAS, 322, 361
Blanton E. L., Schmidt B. P., Kirshner R. P., Ford C. H., Chromey F. R., Herbst W., 1995, AJ, 110, 2868
Boles T., Beutler B., Li W., Qiu Y. L., Hu J. Y., 2003, IAU Circ. 8062, 1
Bottinelli L., Gouguenheim L., Paturel G., de Vaucouleurs G., 1985, A&AS, 59, 43
Bottinelli L., Gouguenheim L., Fouque P., Paturel G., 1990, A&AS, 82, 391
Cappellaro E., Barbon R., Turatto M., 2003, in Marcaide J. M., Weiler K. W., eds., Proc. IAU Coll. 192, Supernovae (10 Years of 1993J). Springer-Verlag, Berlin, in press
Catchpole R. M. et al., 1987, MNRAS, 229, 15P
Catchpole R. M. et al., 1988, MNRAS, 231, 75P
Catchpole R. M. et al., 1989, MNRAS, 237, 55P
Chugai N. N., Utrobin V. P., 2000, A&A, 354, 122
Ciatti F., Rosino L., 1977, A&A, 56, 59
Clocchiatti A., Phillips M. M., Spyromilio J., Leibundgut B., 2001, in Suntzeff N. B., Phillips M. M., eds, SN 1987A: Ten Years After. Astron. Soc. Pac., San Francisco
de Mello D., Benetti S., 1997, IAU Circ. 6537
Dimai A., Li W., 1999, IAU Circ. 7335
Ekholm T., Lanoix P., Teerikorpi P., Fouquè P., Paturel G., 2000, A&A, 355, 835
Elliott K. H., Blades J. C., Zealey W. J., Tritton S., 1978, Nat, 275, 198
Elmhamdi A. et al., 2003, MNRAS, 338, 939
Evans R., Quirk. S., 2003, IAU Circ. 8042
Filippenko A. V., Stern D., Reuland M., 1999, IAU Circ. 7043
Fisher A., 2000, PhD thesis, Univ. Oklahoma
Fouquè P., Solanes J. P., Sanchis T., Balkowski C., 2000, A&A, 375, 770
Freedman W. L. et al., 2001, ApJ, 553, 47
Garcia A. M., 1993, A&AS, 100, 47
Garnavich P., Jha S., Challis P., Kirshner R., Calkins M., 1999a, IAU Circ. 7143
Garnavich P., Jha S., Kirshner R., Challis P., Schmidt B., 1999b, IAU Circ. 7304
Gilmore G., 1978, IAU Circ. 3221

Giovanelli R., Haynes M. P., Herter T., Vogt N. P., Wegner G., Salzer J. J., da Costa L. N., Freudling W., 1997, AJ, 113, 22
Giuricin G., Marinoni C., Ceriani L., Pisani A., 2000, ApJ, 543, 178
Hamuy M., 2003, ApJ, 582, 905
Hamuy M., Walker A. R., Suntzeff N. B., Gigoux P., Heathcote S. R., Phillips M. M., 1992, PASP, 104, 533
Hamuy M., Suntzeff N. B., Heathcote S. R., Walker A. R., Gigoux P., Phillips M. M., 1994, PASP, 106, 566
Hamuy M. et al., 2001, ApJ, 553, 886
Höflich P., Wheeler J. C., Wang L., 1999, ApJ, 521, 179
Hurst G. M. et al., 2001, IAU Circ. 7662
Iwamoto K. et al., 1998, Nat, 395, 672
Jeffery D. J., Branch D., 1990, in Wheeler J. C., Piran T., Weinberg S., eds, Jerusalem Winter School for Theoretical Physics Vol. 6, Supernovae. World Scientific, Singapore, p. 90
King J. Y., 1999, IAU Circ. 7141
Kraan-Korteweg R. C., 1986, A&AS, 66, 255
Landolt A. U., 1992, AJ, 104, 340
Leonard D. C. et al., 2002a, PASP, 114, 35
Leonard D. C. et al., 2002b, AJ, 124, 2490
Leonard D. C., Kanbur S. M., Ngeow C. C., Tanvir N. R., 2003, ApJ, 594, 247
Li W., 1999, IAU Circ., 7143, 3
Matheson T., Jha S., Challis P., Kirshner R., Calkins M., 2001, IAU Circ. 7583
Matheson T., Challis P., Kirshner R., Calkins M., 2003, IAU Circ. 8063
Mattila S., Meikle W. P. S., 2001, MNRAS, 324, 325
Menzies J. W. et al., 1987, MNRAS, 227, 39
Mueller J., Brewer C., Cappellaro E., della Valle M., 1993, IAU Circ. 5784
Nakano S., Aoki M., 1999, IAU Circ. 7304
Pastorello A., Ramina M., Zampieri L., Navasardyan H., Salvo M., Fiaschi M., 2003, in Marcaide J. M., Weiler K. W., eds, Proc. IAU Coll. 192, Supernovae (10 Years of 1993J). Springer-Verlag, Berlin, in press
Patat F., Barbon R., Cappellaro E., Turatto M., 1994, A&A, 282, 731
Patat F., Benetti S., Cappellaro E., Rizzi L., Turatto M., 1999, IAU Circ. 7183
Patat F. et al., 2001, ApJ, 555, 900
Pooley D. et al., 2002, ApJ, 572, 932
Popov D. V., 1992, Sov. Astron. Lett., 18, 59
Qian Y.-Z., Wasserburg G. J., 2002, ApJ, 123, 678
Richardson D., Branch D., Cesebeer D., Millard J., Thomas R. C., Baron E., 2002, AJ, 123, 745
Richmond M. W. et al., 1996, AJ, 111, 327
Ruiz-Lapuente P., Canal R., Kidger M., Lopez R., 1990, AJ, 100, 782
Schaefer B. E., 1996, ApJ, 464, 404
Schlegel D. J., Finkbeiner D. P., Davis M., 1998, ApJ, 500, 525
Schmidt B. P. et al., 1994, AJ, 107, 1444
Sersic J. L., 1973, PASP, 85, 103
Smith R. C., Wells L., della Valle M., Bouchet P., 1992, IAU Circ. 5638
Sollerman J., 2002, NewAR, 46, 493
Sollerman J., Cumming R. J., Lundqvist P., 1998, ApJ, 493, 933
Sollerman J., Kozma C., Fransson C., Leibundgut B., Lundqvist P., Ryde F., Woudt P., 2000, ApJ, 537, 127
Stone R. P. S., 1977, ApJ, 218, 767
Stone R. P. S., Baldwin J. A., 1983, MNRAS, 204, 237
Storchi-Bergmann T., Eracleous M., Ruiz M. T., Livio M., Wilson A. S., Filippenko A. V., 1997, ApJ, 489, 87
Strolger L.-G., Seguel J. C., Krick J., Block A., Candia P., Smith R. C., Suntzeff N. B., Phillips M. M., 2000, IAU Circ. 7524
Szabo R., 1999, IAU Circ. 7193
Turatto M., Cappellaro E., Barbon R., Della Valle M., Ortolani S., Rosino L., 1990, AJ, 100, 771
Turatto M., Cappellaro E., Benetti S., Danziger I. J., 1993, MNRAS, 265, 471
Turatto M., Gouiffes C., Leibundgut B., 1994, IAU Circ. 5987
Turatto M. et al., 1998, ApJ, 498, 129
Weisz D., Modjaz M., Li W. D., 2001, IAU Circ. 7579
West R. M., Lauberts A., Jorgensen H. E., Schuster H. E., 1987, A&A, 177, 1
Whitelock P. A. et al., 1988, MNRAS, 234, 5
Whitelock P. A., Feast M. W., Catchpole R. M., 1989, MNRAS, 238, 7
Wolstencroft R. D., Tully R. B., Perley R. A., 1984, MNRAS, 207, 889
Woosley S. E., Weaver T. A., 1995, ApJS, 101, 181
Woosley S. E., Pinto P. A., Martin P. G., Weaver T. A., 1987, ApJ, 318, 664
Young T. R., Baron E., Branch D., 1995, ApJ, 449, 51
Zampieri L., Shapiro S. L., Colpi M., 1998a, ApJ, 502, 149
Zampieri L., Colpi M., Shapiro S. L., Wasserman I., 1998b, ApJ, 505, 876
Zampieri L., Pastorello A., Turatto M., Cappellaro E., Benetti S., Altavilla G., Mazzali P., Hamuy M., 2003, MNRAS, 338, 711
Zealey W., Tritton S., 1978, IAU Circ. 3224

This paper has been typeset from a TEX/LATEX file prepared by the author.